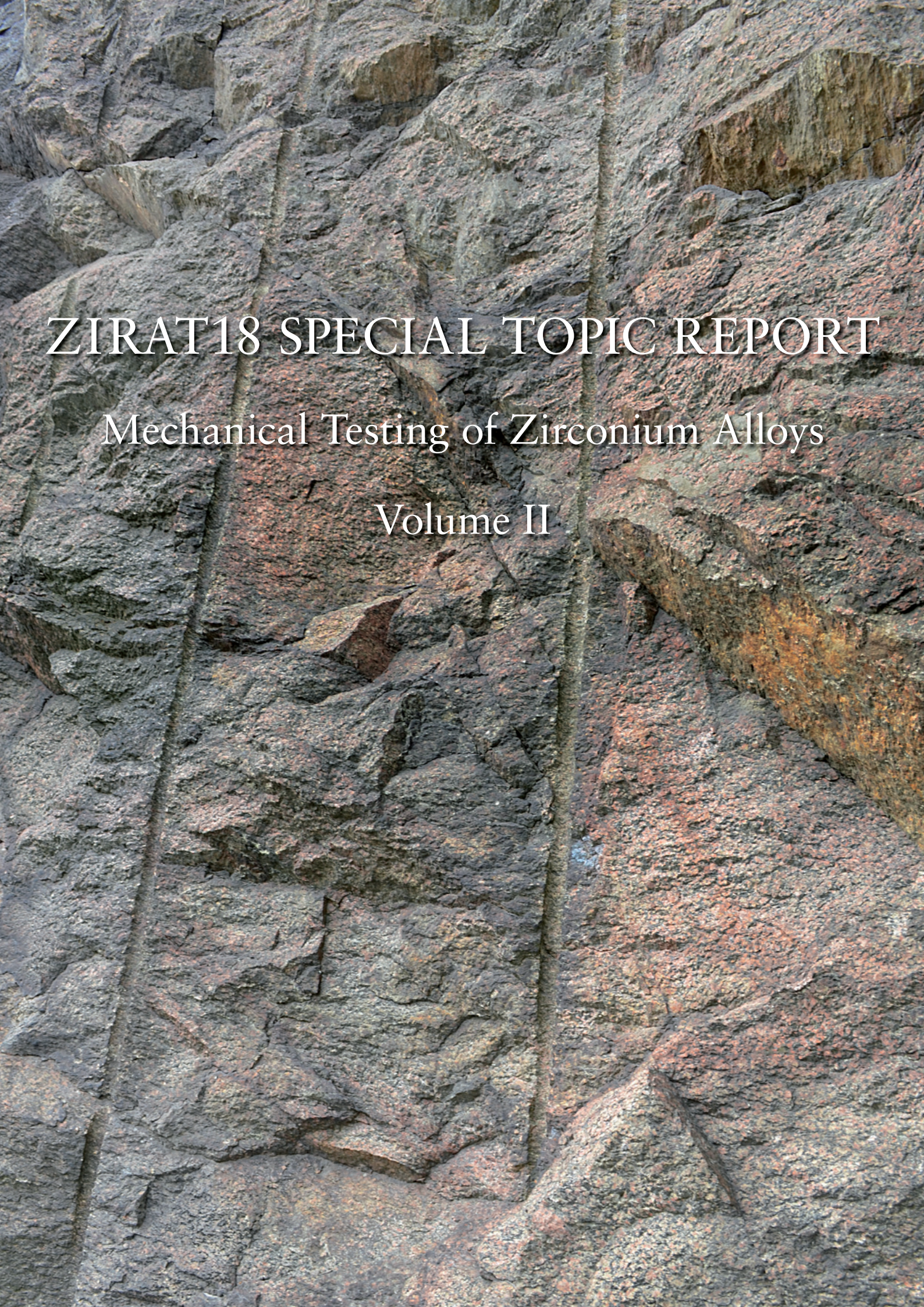

# ZIRAT18 SPECIAL TOPIC REPORT

## Mechanical Testing of Zirconium Alloys

## Volume II

# Mechanical Testing of Zirconium Alloys

# Volume II

*Authors*

Ron Adamson
Fremont, CA, USA

Peter Rudling
ANT International, Mölnlycke, Sweden

Kit Coleman
Deep River, ON, Canada

Tahir Mahmood
Pleasanton, CA, USA

*Technical Editor*

Ron Adamson
Fremont, CA, USA

A.N.T. INTERNATIONAL®


Advanced Nuclear Technology International
Analysvägen 5, SE-435 33 Mölnlycke
Sweden

info@antinternational.com
www.antinternational.com


Ecolabelled printed matter, 441 799

# Disclaimer

The information presented in this report has been compiled and analysed by Advanced Nuclear Technology International Europe AB (ANT International®) and its subcontractors. ANT International has exercised due diligence in this work, but does not warrant the accuracy or completeness of the information. ANT International does not assume any responsibility for any consequences as a result of the use of the information for any party, except a warranty for reasonable technical skill, which is limited to the amount paid for this assignment by each ZIRAT/IZNA programme member.

# Contents

# 1 Introduction (Ron Adamson and Peter Rudling)

Mechanical testing of zirconium alloys has many uses: to confirm that the material meets the specification, to evaluate new alloys or modifications to old ones, to elucidate mechanisms of strengthening or embrittlement, and to assess the effects of reactor operation. The mechanical response of any material depends on several different parameters such as:

1) Specimen geometry,
2) Alloy composition and microstructure,
3) Loading conditions such as stress state and strain rate, and
4) Environment such as temperature, irradiation and ambient chemistry.

Residence in a nuclear reactor presents a severe test for materials. Before evaluating the mechanical properties, knowledge is required on the conditions of normal reactor service with its operational variations, the challenge when spent fuel is stored, and the consequences of accidents. Various mechanical tests are done to simulate the conditions faced by fuel cladding and structural components in the reactor. In applying the results from mechanical testing of zirconium alloys to reactor performance, it is crucial to have a good knowledge of the situation being addressed and how the different critical testing parameters affect the material response so the results are useful to predict performance accurately and satisfy regulatory requirements. The objective of this STR in two volumes is to provide this knowledge.

This report is Volume 2 of a two-part Special Technical Report (STR) on mechanical testing of zirconium alloys. Volume 1 deals with separate effects testing, and volume 2 deals with integral or specific phenomena testing. Background information will be included where appropriate, but an extensive literature review of specific performance is not intended.

## 1.1 Fuel design requirements

The objectives of the *fuel system* safety review are to provide assurance that:

1) The *fuel system* is *not damaged* as a result of normal operation and AOOs.
    a) Fuel system consists of assemblies of fuel rods including fuel pellets, insulator pellets, springs, tubular cladding, end closures, hydrogen getters, and fill gas; burnable poison rods including components similar to those in fuel rods; hold-down spring, connections, spacer grids and springs; end plates; channel boxes; and reactivity control elements that extend from the coupling interface of the control rod drive mechanism in the core.
    b) Not damaged means not only that the fuel integrity is maintained, i.e., no release of radioactivity, but also that the fuel system dimensions remain within operational tolerances, and that functional capabilities are not reduced below those assumed in the safety analysis. This objective implements General Design Criterion 10 (GDC10) and the design limits that accomplish this are called Specific Acceptable Fuel Design Limits (SAFDLs).
2) *Fuel system* damage is never so severe as to prevent control rod insertion when it is required.
3) The number of *fuel rod failures* is not underestimated for postulated accidents.
    a) Fuel rod failure means that the fuel cladding has been breached and radioactivity from the fuel get access to the coolant.
4) *Coolability* is always maintained.
    a) Coolability means that the FA retains its rod-bundle geometry with adequate coolant to permit removal of residual heat even after a severe accident.

Objective (1) in the above list is formalized in GDC10 [10 CFR Part 50 Appendix A, 1990]. The application of *GDC10* is described in the SRP [USNRC, 2007]. The *fuel system,* nuclear, and thermal and hydraulic designs are covered in SRP Sections 4.2, 4.3 and 4.4, respectively. Section 4.2 in SRP identifies a number of *fuel system* failure mechanisms that actually have occurred in commercial reactors, as well as hypothesized *fuel system* failure mechanisms. For each of these *fuel system* failure mechanisms, SRP Section 4.2 lists a corresponding design limit intended to accomplish objective (1) in the list above. These design limits are called SAFDLs. Thus, the SRP does not include any design limits to address potential new *fuel system* failure mechanisms related to more recent fuel designs and/or reactor operation strategies.

Fuel rod failures must be accounted for in the dose analysis required by [10 CFR Part 100, 1995], for postulated accidents.

The general requirements to maintain control rod insertability and core coolability appear in the General Design Criteria, e.g., GDC 27 and GDC 35. Specific coolability requirements for the loss of coolant accidents, LOCA, are provided in [10 CFR Part 50, §50.46].

The *fuel system* design bases must take the four objectives described on the previous page into account. The SAFDLs discussed below do this. In a few cases the SAFDLs provide the design limit but in most cases it is up to the fuel vendor to recommend a design limit value, taking a specific failure mechanism into account. The fuel vendor must also provide the background data for the design limits (that are specified by the NRC as well as those used by the specific fuel vendor) to ensure that the design limit is both necessary and sufficient. The fuel vendor must also provide data for the specific fuel design that shows that the design limit is met to get their fuel licensed.

Specific failure mechanisms for the *fuel system (including the fuel rod)* and licensing criteria related to classes I and II operation and classes III and IV events are discussed in the following subsections.

The pertinent mechanical tests related to fabrication and in-pile performance issues are summarised in Table 1-1. These mechanical tests will be discussed in detail in the following sections of the report.

In the following Section 1.2, only the design criteria related to mechanical properties of the zirconium alloy fuel components are discussed during normal operation and AOO, DBA and Dry Storage.

Table 1-1: Relevant mechanical tests for fabrication and in-pile performance issues

| | Fabrication Issues | | In-Pile Issues | |
|---|---|---|---|---|
| **Component** | **Operation** | **Properties** | **Service Condition** | **Property** |
| **Spacer** | Bend<br>Punch<br>Cold roll | UE[1], TE[2]<br>UE, TE<br>UE, FT | Seismic, Handling<br><br>Vibration<br>Dimensions | IS[3], TE, FT[4]<br><br><br>F[5], H[6]<br>IG[7] |
| **Channel** | Bend<br>Cold roll | UE, TE<br>UE, TE, FT | Seismic, Handling<br>Vibration<br>Wear | IS TE, FT<br>IS TE, FT<br>F<br>H |
| **Water rod/guide tube** | Cold reduce | UE, TE, FT | Handling<br>Assembly support | TE, S[8], IS, FT<br><br>S, TE, FT |
| **Spacer (grid) spring** | Cold roll | TE, UE | Vibration<br>Wear<br>Relaxation | F<br>H<br>IG, C[9] |
| **Tubing** | Cold roll | TE, UE, FT | Thermal stress<br>PCI<br><br>Length, bow<br>Differential pressure | F<br>UW, IGSCC[10], LME[11]<br>IG, C, S<br>S, C, UE, B[12] |
| | | | | ANT International, 2013 |

[1] Uniform elongation
[2] Total elongation
[3] Impact strength
[4] Fracture toughness
[5] Fatigue
[6] Hardness
[7] Irradiation growth
[8] Strength
[9] Creep
[10] Iodine assisted stress corrosion cracking
[11] Cadmium liquid metal embrittlement
[12] Burst strength

# 1.2 Normal operation and Anticipated Operational Occurrences (AOO)

## 1.2.1 Fuel system damage

A fuel component is considered as failed according to SRP if the component does not comply with the fuel design criteria. Thus, a fuel assembly that exhibits more dimensional changes than the fuel design criterion on dimensional stability specifies, the fuel assembly is considered as failed even though the fuel rods may be intact.

### 1.2.1.1 Stress, strain or loading limits

Stress, strain and loads must be limited for space grids, guide tubes, fuel rods, control rods, channel boxes and other *fuel system* structural members or otherwise the component may fail. Stress limits that are obtained by methods similar to those given in Section III of the ASME Code, see Section 1.2.1.1, [ASME, 2010] are acceptable. Other proposed limits must be justified.

#### 1.2.1.1.1 Stress limit

Plastic deformation is regarded as material failure according to the ASME Code, and must therefore not occur. *This requirement is fictitious since creep deformation is plastic deformation and creep limited strain is allowed.*

Stresses in the *fuel system* structural members may be categorised depending on the origin of the stress and on the geometrical and material discontinuities at the point in the *fuel system* structural member where the stress is calculated.

The ASME Code and comparable design verification systems describe what category of stresses must be taken into account and also how the equivalent stress for each stress category should be evaluated. The design verification systems also specify the maximum allowable equivalent stress in each stress category. The following stress categories, $C_i$, are defined according to the ASME, [ASME, 2010], and KTA [KTA, 2013][13], design specifications.

$C_1 = P_m$ = Primary Membrane Stress

Primary stresses are stresses originating from applied loads such as e.g. cladding stresses due to a fuel rod internal overpressure. Primary stresses are not self-limiting and if the yield stress in the component is exceeded, plastic deformation in the whole material thickness will occur. In the case of a fuel rod this would mean that the whole cladding thickness would plastically deform.

Membrane stress are stresses which have a constant value in the whole material thickness, which means that if the yield stress is exceeded, plastic deformation will occur simultaneously in the whole material thickness.

$C_2 = P_m + P_b$ = Primary Membrane + Primary Bending Stress

Bending stresses will result in varying stress levels in the material thickness and when the yield strength is exceeded only local plastic deformation occurs.

[13] http://www.kta-gs.de/d/regeln/3100/3103_re_2012_11.pdf

$C_3 = P_m + P_b + Q$ = Primary and Secondary Membrane + Bending Stress

Secondary stresses relates to stresses resulting from incompatibility between different volume elements in a component, e.g., caused by a radial temperature gradient in the fuel rod cladding. The secondary stresses are self-limiting, i.e., the stress will relax if the yield strength is exceeded casing the material to locally plastically deform. Examples of secondary stresses are thermal and bending stresses.

The Japanese Guidebook of Safety Assessment and Review, JGSAR, [Motta, 1995] define the following stress categories:

$C_1$ = Primary Stress

$C_2$ = Secondary Stress

According to the ASME Code, the Tresca formula should be used to calculate the equivalent stress as follows:

$$\sigma_e = \max\left(|\sigma_{11} - \sigma_{22}|, |\sigma_{22} - \sigma_{33}|, |\sigma_{33} - \sigma_{11}|\right)$$

where

$\sigma_{11}$, $\sigma_{22}$, $\sigma_{33}$ are the principal stresses.

However, according to the KTA and JGSAR Codes of design, the equivalent stress shall be calculated by the von Mises formula, as follows:

$$\sigma_e = \frac{1}{\sqrt{2}}\left[(\sigma_{11} - \sigma_{22})^2 + (\sigma_{22} - \sigma_{33})^2 + (\sigma_{33} - \sigma_{11})^{\frac{1}{2}}\right]$$

For each stress category $C_i$, let the allowable stress be given by $S_i$ and let *Y(T)* and *U(T)* represent the yield strength and the ultimate strength in unirradiated condition, respectively.

The KTA Code specifies that

$$S_1 = \min(0.90Y(T), 0.5U(T))$$
$$S_2 = \min(1.35Y(T), 0.7U(T))$$
$$S_3 = \min(0.90Y(T), 0.50U(T))$$

$S_3$ =min (2.7Y(T), 1.0U(T)

and the ASME Code states that

$$\begin{matrix} S_1 = 1.0S_m \\ S_2 = 1.5S_m \\ S_3 = 3.0S_m \end{matrix} \text{ where } S_m = \min\left(\begin{matrix} Y(T_0)/1.5 \\ Y(T)/1.5 \\ U(T_0)/3 \\ U(T)/3 \end{matrix}\right) \text{ and } T_0 = 20^oC$$

while the JGSAR design specification requires that

$$S_1 = Y(T)$$
$$S_2 = U(T)$$

The design specification then states that the equivalent stress of the combination of the different stresses $\sigma_e^{max}$ in a given stress category $C_i$ must not exceed the maximum allowable stress $S_i$ for the particular stress category, i.e.

$$\left(\sigma_e^{max}\right)_{C_i} \leq S_i$$

It is important to keep in mind that this design stress criterion is very conservative since material properties in unirradiated condition must be used in the above described calculations. However, the yield strength and the ultimate strength material values are dramatically increased during the first couple of months of irradiation, thus increasing the margin on the maximum allowable stress (Figure 1-1).

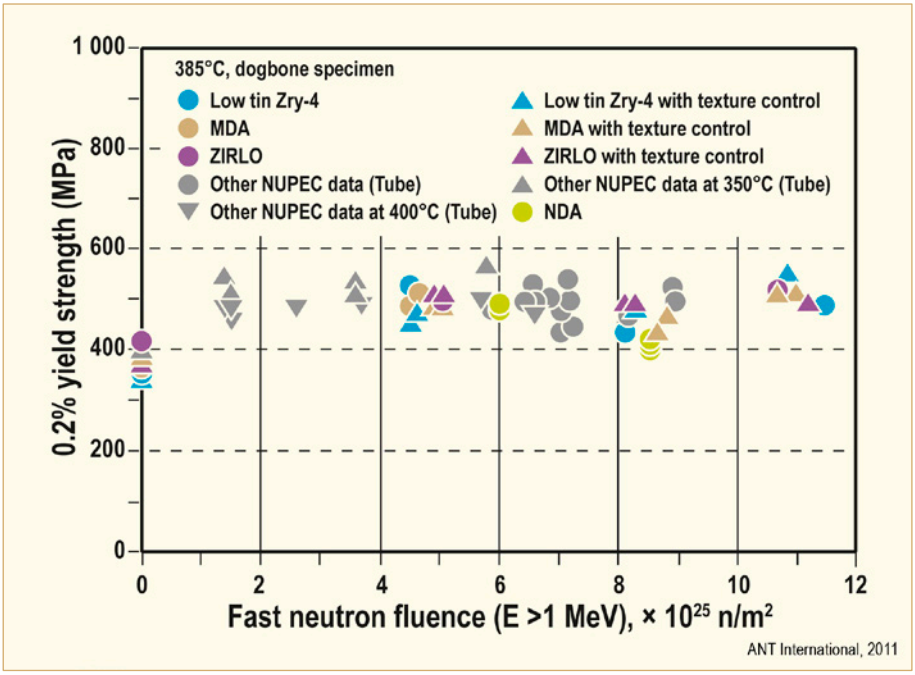


Figure 1-1: Relation between fast neutron fluence and yield strength at 385°C for various Nb-containing and Zry alloys. A fast neutron fluence of $2 \cdot 10^{25}$ n/m$^2$ corresponds to a burnup of about 5 GWd/MT, after [Tsukuda et al, 2003] and [Goto et al, 2000].

This design stress criterion is the reason for selecting a higher strength fuel cladding material for PWRs compared with BWRs. The fuel cladding stresses are much higher in the former case due to a larger system-rod differential pressure. Therefore, Stress Relieved Cladding, SR, Zry-4 or Zry-2 with a much higher strength was needed historically in PWRs while a softer, Recrystallized, RX, material could be used for BWRs. Since Nb additions to Zirconium have a significant solution hardening effect[14], materials such as M5, Zr1Nb, can be used in PWRs in the RX state.

[14] 40 MPa/% Nb, independent of T.

#### 1.2.1.1.2 Strain limit

At stresses below the yield strength, the material may deform during irradiation due to creep deformation. The SR does not specify a specific creep strain limit.

**Design criterion –** For BWR fuel rods a maximum allowable equivalent plastic creep strain of 2.5%, corresponding to about 1.5% plastic tangential strain, is sometimes used by fuel vendors (in Germany and Sweden). The initial creep down of the cladding due to larger system than rod internal pressure is not taken into account. Only the outward creep strain after pellet/cladding contact has occurred is compared to the limit. This outward creep is due to pellet swelling during irradiation and occurs at a very slow rate.

For PWRs a maximum allowable creep strain corresponding to a 1% increase in fuel rod diameter compared to the initial diameter is often used (for example, in Sweden, France, the Netherlands, and Switzerland). This limit is related to the risk of getting DNB if the diameter increase becomes too large to permit the coolant to effectively remove heat from the fuel rod; i.e., a small change comes from CHF $\propto (D_{rod})^{-0.5}$, so that a 1% increase in diameter corresponds to about a 0.5% decrease in CHF, while larger changes are postulated to result from cladding deformation due to lift-off, disruption of heat transfer and the propagation of DNB and lift-off conditions among adjacent fuel rods.

### 1.2.1.2 Fatigue limit

Fatigue stresses may be induced in the fuel assembly components due to, e.g., the turbulent coolant flow.

According to the SRP, the cumulative number of strain fatigue cycles on the structural components should be significantly less than the design fatigue lifetime, which is based upon the data by O'Donnell and Langer, [O'Donnell & Langer, 1964], and includes a safety factor of 2 on stress amplitude or a safety factor of 20 on the number of cycles. Other proposed limits may be used but must be justified according to the SRP.

In design calculations the fuel vendor must show that alternating bending stresses due to dynamic loads must be below $\pm$ 50 MPa.

Normally the dynamic stress is much below $\pm$ 50 MPa in the structural components and therefore there is a lot of safety margin regarding fatigue failures.

## 1.2.2 Fuel rod failure

SRP states that to meet the requirements of:

- GDC10 as it relates to SAFDLs for normal operation and anticipated operational occurrences and,
- 10CFR Part 100 as it relates to fission product release for postulated accidents,

*fuel rod* design criteria should be given for all known *fuel rod failure*[15] mechanisms.

Different *fuel rod failure* mechanisms that are related to mechanical properties of the claddings are discussed in the following. As was the case for the fuel systems, it is mostly up to the fuel vendor to define a criterion for each fuel rod failure mechanism listed in the SRP to ensure that this failure mechanism will not occur during normal operation and anticipated operational occurrences. In some cases SRP provides the fuel rod design criterion.

[15] Fuel rod failure occurs when the fuel cladding has lost its integrity and radioactive fission products may be released to the coolant.

### 1.2.2.1 Cladding collapse

At the start of irradiation the system pressure is larger than the rod internal pressure, resulting in compressive stresses in the fuel cladding. If these stresses become large enough, the cladding tube may either instantaneously buckle elastically or, if the stresses exceed the yield strength, collapse due to plastic deformation. To prevent elastic buckling and plastic deformation, the fuel vendor has to show by calculations that the fuel cladding stresses are below those resulting in elastic buckling or plastic deformation. Fuel rod failure due to elastic buckling or plastic collapse has never been observed in commercial nuclear reactors. A more limiting condition that has been observed in commercial PWR nuclear reactors is cladding creep collapse. This condition occurs at cladding stresses far below that required for elastic buckling or plastic deformation.

In the early 1970s, excessive in-reactor fuel pellet densification resulted in the production of large fuel column pellet-pellet axial gaps in some PWR fuel rods. The high PWR coolant pressure in conjunction with the thin PWR cladding tubes and low fill gas pressure resulted in excessive fuel rod cladding creep rates and subsequent cladding collapse over fuel column axial gaps. Such collapse occurs due to a slow increase of cladding initial ovality due to the cladding creep noted above. The creep results from the combined effect of reactor coolant pressure, temperature and fast neutron flux on the cladding over the axial gap. Since the cladding is unsupported by fuel pellets in the axial gap region, the ovality can become large enough to result in elastic instability and cladding collapse.

While axial gaps can be prevented (or detected) in as-fabricated fuel, the potential formation of gaps during operation cannot be controlled. Thus the vendor must show that the fuel cladding will not collapse, either elastically, plastically or by creep. Elastic and plastic collapse is most limiting at Beginning of Life (BOL) before irradiation hardening of the cladding. Creep collapse becomes limiting later in life.

According to the SRP, a collapsed cladding must be regarded as a failed fuel rod due to the large strains that result from cladding collapse.

Note that in CANDU reactors the Zircaloy-4 fuel cladding is designed to collapse onto the fuel to provide good heat-transfer to the heat-transport heavy water. In this fuel the filler gas, He, is initially at atmospheric pressure.

### 1.2.2.2 Pellet/Cladding Interaction, PCI

According to the SRP, there is no current criterion for fuel failure resulting from PCI. Two related criteria should be applied, but they are not sufficient to preclude PCI failures:

- The transient induced uniform elastic and plastic strain should not exceed 1%. Since PCI failures may occur at lower strains than 1%, this criterion is not sufficient to ensure the non-occurrence of PCI failures. The basis for the 1% criterion is unknown, even to the R&D branch of NRC, [Meyer, 1999].
- Fuel pellet melting should be avoided.

# 2 Secondary degradation of failed fuel (Peter Rudling)

The interested reader is referred to ZIRAT13/IZNA8 STR Vol. II

## 2.1 Primary failures causes

There are a number of primary fuel failure causes that have been recorded for BWR and PWRs fuel since the early days of operation, as listed in Table 2-1. More information on primary defects can be obtained from e.g. Section 4 in the FMTR Vol. I [Cox et al, 2006].

Table 2-1: Known primary failure causes for BWR and PWR fuel rods.

| Primary Failure Cause | Short Description |
|---|---|
| Manufacturing defects | Non-through-wall cracks in the fuel cladding developed during the cladding manufacturing process may propagate through the whole cladding thickness during a power ramp by a PCMI mechanism.<br>Defects in bottom and/or top end plug welds.<br>Primary hydriding due to moisture in fuel pellets and or contamination of clad inner surface by moister or organics.<br>Too large gap between the fuel rod and the spacer grid supports leading to excessive vibrations in the PWR fuel resulting in grid-rod fretting failures.<br>Chipped pellets or pellets with “missing surfaces” may result in PCI failures |
| Excessive Corrosion | Accelerated corrosion resulting in cladding perforation.<br>This corrosion acceleration can be generated by water chemistry impact such as e.g. CRUD deposition or thermo hydraulic impact leading to (DNB). DNB may be related to excessive fuel rod or fuel assembly bowing. |
| Fuel Assembly Bowing | Fuel assembly bowing is due to excessive fuel assembly holding down forces that may be due to excessive guide tube growth by hydriding (from the hydrogen released through the corrosion reaction between the coolant and the zirconium clad material) and irradiation growth.<br>Fuel assembly bowing may result in difficulties to insert the control rods (a safety issue) and/or decreased thermal margins (LOCA and DNB). Excessive bowing may also result in grid-grid fretting and difficulties in fuel assembly handling during the outage. |
| PCI | PCI -an iodine assisted stress corrosion cracking phenomenon that may result in fuel failures during rapid power increases in a fuel rod. This failure mechanism is occurring much more frequent in BWRs but have also occurred in PWRs. There are three components that must occur simultaneously to induce PCI and they are: 1) tensile stresses- induced by the power ramp, 2) access to freshly released iodine-occurs during the power ramp and, 3) a sensitised material – Zircaloy is normally sensitive enough for iodine stress corrosion cracking even in unirradiated state. |
| Cladding collapse | This failure mechanism occurred in earlier days due to pellet densification. This failure mode has today been eliminated by fuel design changes and improved manufacturing control. |
| Fretting | This failure mode has occurred due to:<br>Debris fretting<br>Grid-rod fretting - Excessive vibrations in the PWR fuel rod causing fuel failures. This situation may e.g. occur due to different pressure drops in adjacent fuel assemblies causing cross-flow. Grid-rod fretting may also occur due to a poor grid design or manufacturing process.<br>Baffle jetting failures - Related to unexpectedly high coolant cross-flows close to baffle joints |
| Dry-out | The local power is too high for the coolant flow, causing the cladding to be overheated. The overheating causes (local) corrosion penetration of the cladding. Only one case known. |
| | ANT International, 2013 |

# 2.2 Degradation of failed fuel

## 2.2.1 Introduction

Degradation of failed fuel is a situation when fuel is dispersed (Figure 2-1). This may occur if the rods cracks to such a point that the water gets in contact with the fuel pellet. Steam will not result in fuel dispersion while the water phase can. Normally, utilities are much more concerned about fuel washout than high iodine and noble gas release. This, since it may take up to 10 years to clean the core from the tramp uranium resulting from the fuel dissolution. On the other hand, the high iodine and noble gas activities released from the failed rod will be eliminated when the failed rod is extracted from the core.

Degradation has historically been more of an issue in BWRs than in PWRs. Failed rods in PWRs may degrade, but the amount of dispersed fuel is lower than that in a BWR. The rationale for the less severe behaviour in PWRs may be due to the fact that the coolant chemistry in a PWR is more reducing than in BWRs. During the period 1992-1993 six plants in US and in Europe were forced into unscheduled outages because of concerns about failed *Zr-sponge liner fuel*[16], [IAEA, no. 388, 1998]. In all these cases, the very high off-gas activities and significant loss of fuel pellet material resulted from only one or two failed rods.

Two different types of degradation scenarios have been identified, namely development of:

- Transversal breaks (also called guillotine cuts or circumferential break) occurring in both BWRs and PWRs/ Voda Voda Energo Reactor (VVERs) (Figure 2-2) and,
- Long axial cracks, i.e. axial splits[17] only occurring in BWRs (but may also occur in PWRs subjected to significant control rod movements during operation), (Figure 2-3).

[16] *Zr sponge liner fuel* consists of a liner produced from Zr sponge material. No alloying elements have been added to this material and its major impurities are oxygen (about 600-900 wtppm) and iron (about 150-500 wtppm).
[17] Axial split is a term introduced by *GE* and represents a failed rod that either has an off gas level larger than 5000 μCi/s (185 MBq/s) or a total crack length that is larger than 152 mm (6 inches).

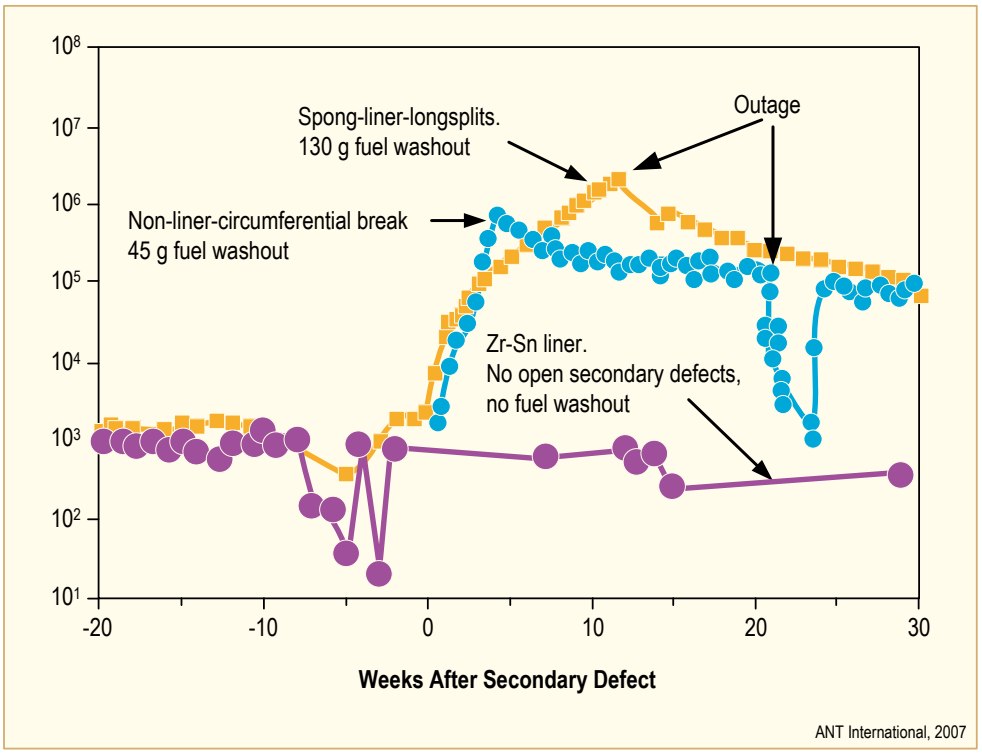


Figure 2-1: 239Np activity (a measure of the $UO_2$ dissolution rate) measured in the coolant before and after formation of: 1) a long split (1 rod with sponge Zr liner-orange data points) and 2) a transversal break (blue data points). A long split cause a significantly larger $UO_2$ dissolution than a transversal break. The violet data points refer to a rod that only had a primary failure and did not degrade. The mass of one fuel pellet is about 7 g. It is also apparent that primary failures normally do not result in fuel dissolution, after [Sihver et al, 1997].

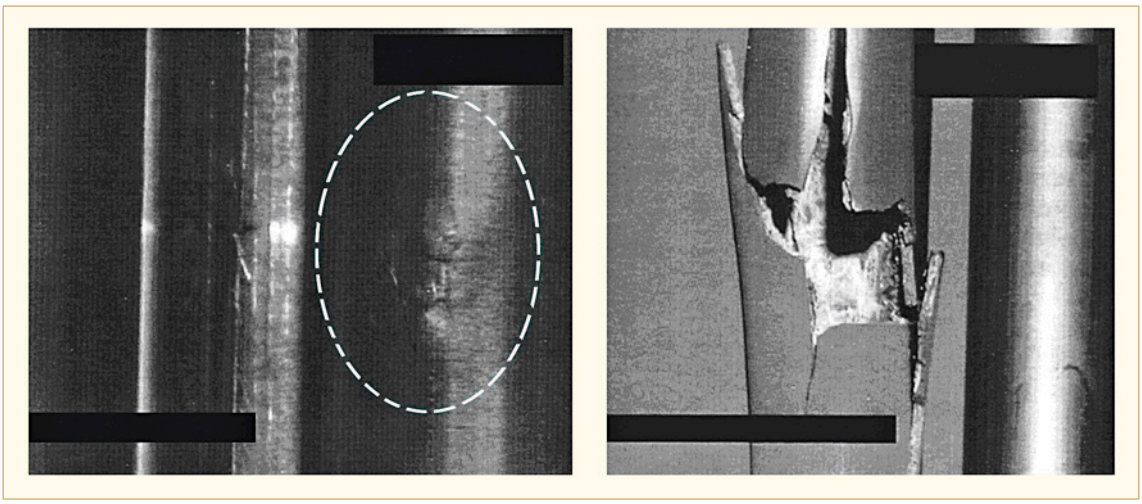

Figure 2-2: Visual inspection of failed rod. Left picture shows the debris fretting failure at spacer no.6, the right picture shows the transversal break between spacer no. 1 and 2.

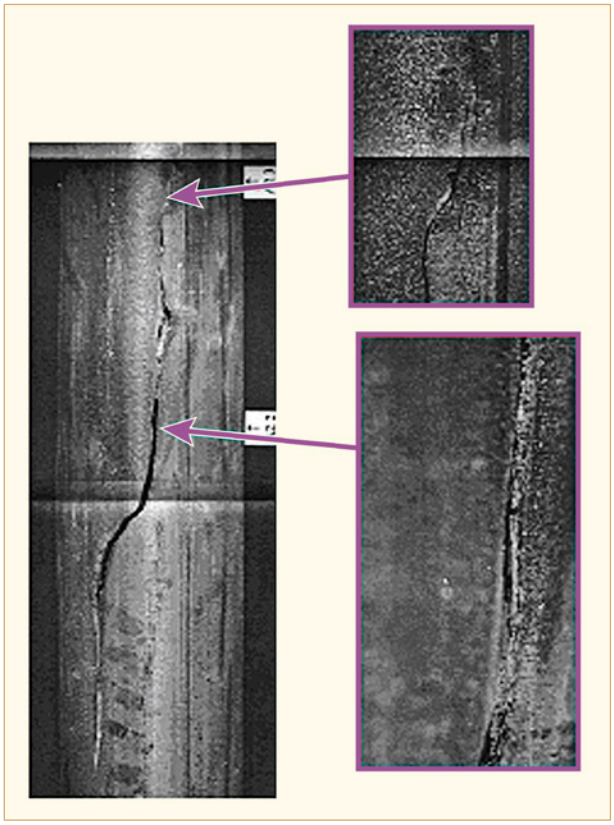

Figure 2-3: Visual inspection of a failed rod showing a long axial crack at the 591-626 mm elevation above the bottom end plug.

## 2.2.2 BWR secondary degradation

Literature data, e.g., [Armijo, 1994] and [Hüttman et al, 1997], shows that axial splits only occur in conjunction with a power ramp of preferentially intermediate to high burnup rods. Thus, if a failed rod is not subjected to a power ramp, no axial split will form. It should be pointed out however, that power ramps must be performed in the reactor for other reasons and consequently, it will be impossible to run a plant without any power ramps.

On the other hand transversal break formation is not correlated to power ramping but can result during operation of a failed rod during constant power, e.g. [Sihver et al, 1997]. Sometimes, it seems that lowering of the reactor power to such an extent that the lower part of the rod may be filled with water, *waterlogging*, such as e.g. during a cold shut-down, may enhance the risk of getting a transversal break upon return to full power. The transversal break tendency is similar for 8x8 and 10x10 fuel designs. It is also noteworthy that the transversal break tendency decreases with burnup level.

Obviously, axial cracks may occur along the whole length of the rod while transversal breaks mostly forms in the bottom part of the failed rod at some minimum distance from the primary defect [Harbottle et al, 1994], (Figure 2-4 and Figure 2-5). However, there are some rare cases when a transversal break has formed at the bottom and top part of a rod with a primary failure in the middle part of the rod.

Based upon the in-pile experience of performance of failed rods, the criteria that have to be fulfilled to get either transversal breaks or axial splits can be identified, see Figure 2-6.

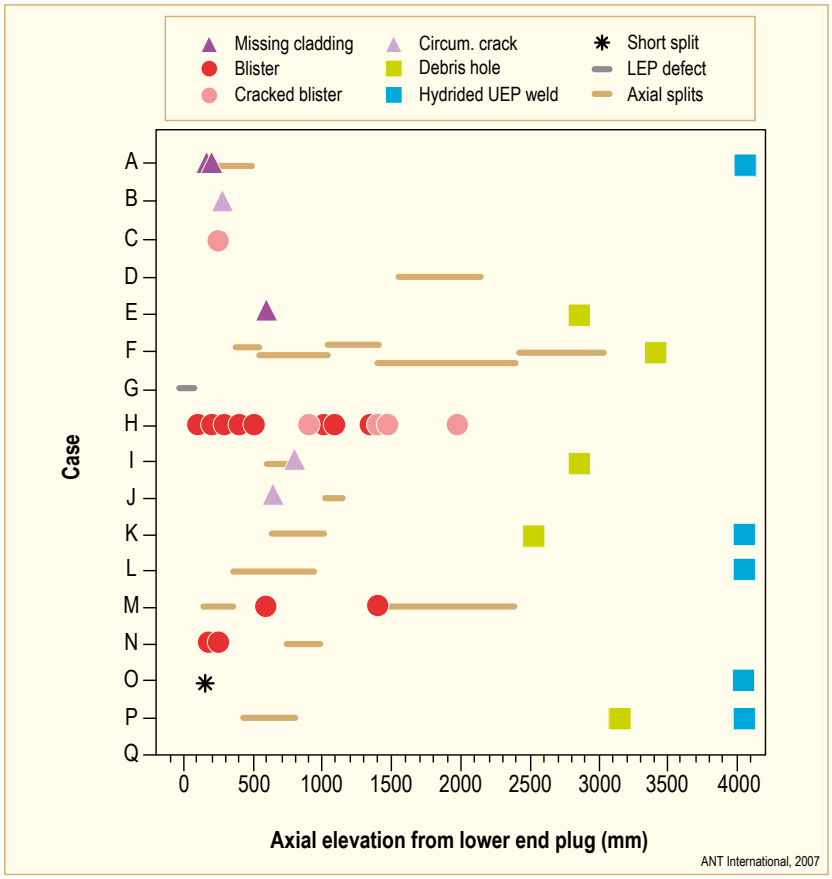


Figure 2-4: Location and dimension of secondary damage in failed GE (now Global Nuclear Fuel (GNF)) and ANF (now AREVA) rods. UEP = Upper End Plug, LEP = Lower End Plug, after [Harbottle et al, 1994].

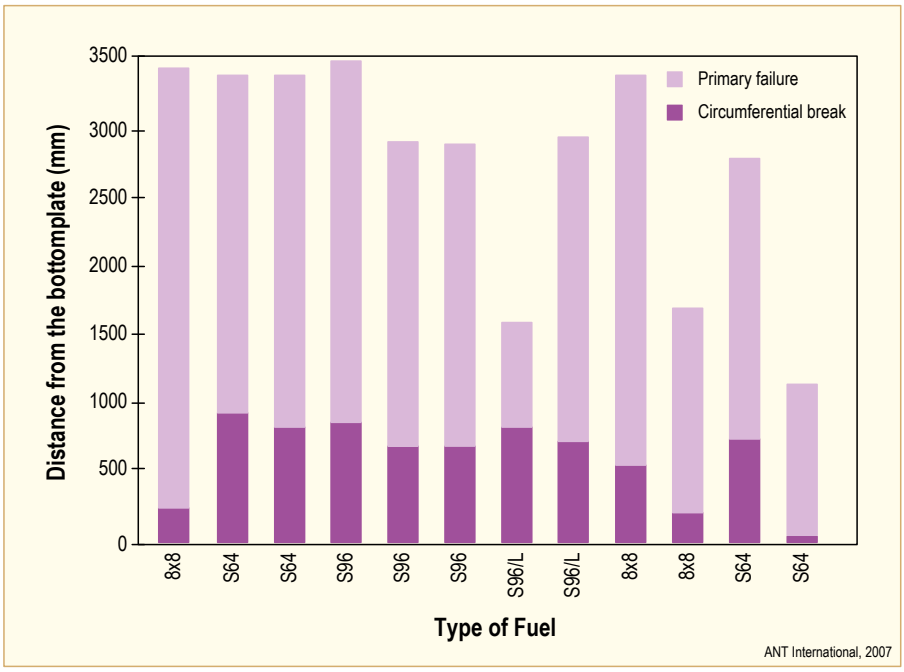


Figure 2-5: Locations of primary failures and transversal breaks, on the fuel rods, for all cases where the exact location of the primary failure has been identified, after [Sihver et al, 1997].

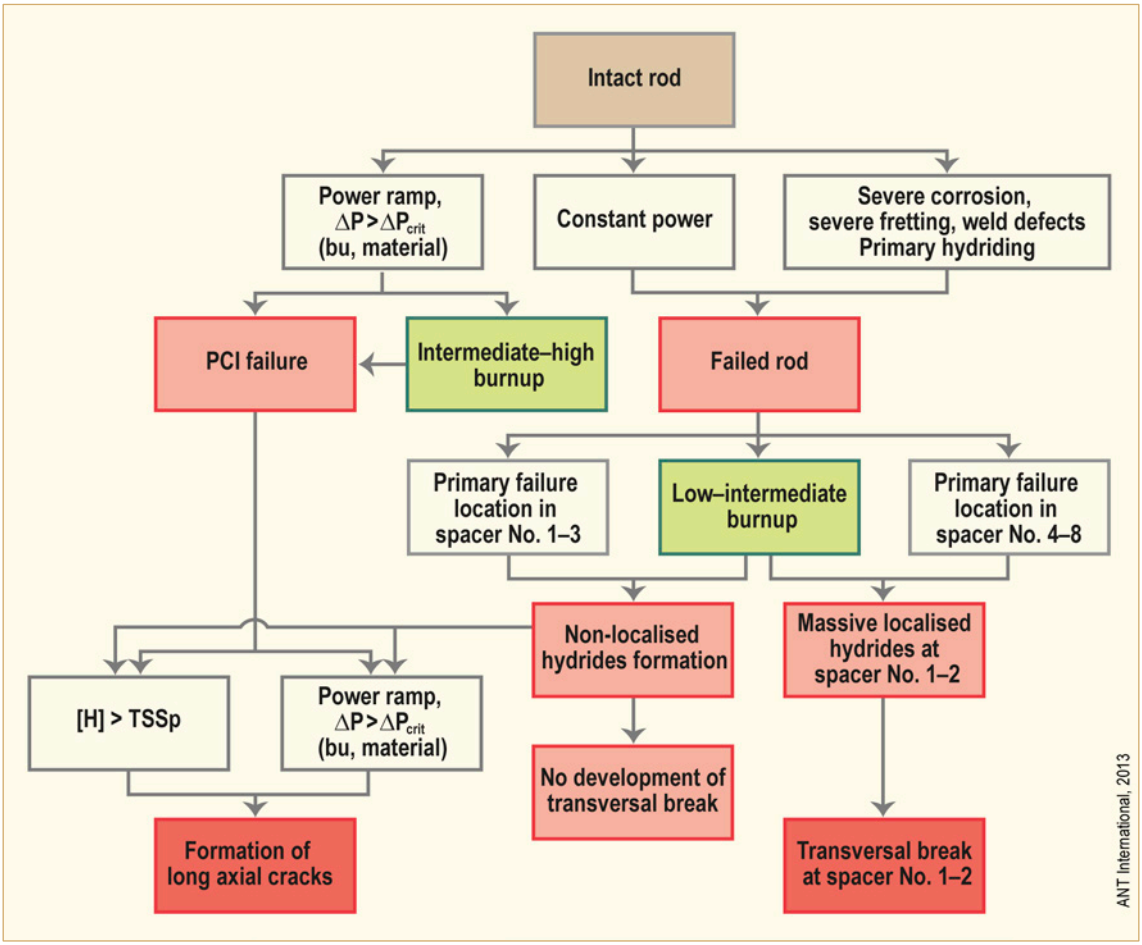


Figure 2-6: Criteria which have to be fulfilled to develop either transversal break or axial splits.

### 2.2.2.1 Transversal break formation

If the failed rod has low to intermediate burnup, one may expect first, that the overall pellet-cladding gap is large and second, that this gap is much smaller at the lower part of the rod due to the downshift in power profile for these rods. Now provided that, at a specific axial rod elevation:

- The ratio of hydrogen to steam partial pressure is large enough and,
- The protecting clad inner surface oxide is thin enough, massive hydrogen ingress into the cladding may occur at this location.

When the hydrogen solid solution solubility has been exceeded, precipitation of hydrides will start with forming *hydride blisters* that subsequently will grow into massive hydrides throughout the cladding thickness along its whole circumference. Since zirconium hydrides are very brittle, the cladding zone that is completely transformed into zirconium hydride will be very brittle and may easily fracture even during operation at constant power.

The events resulting in a transversal break is schematically shown in Figure 2-7, and the parameters impacting the transversal break tendency is shown in Figure 2-8 and is described more in Appendix A, [Strasser et al, 2008].

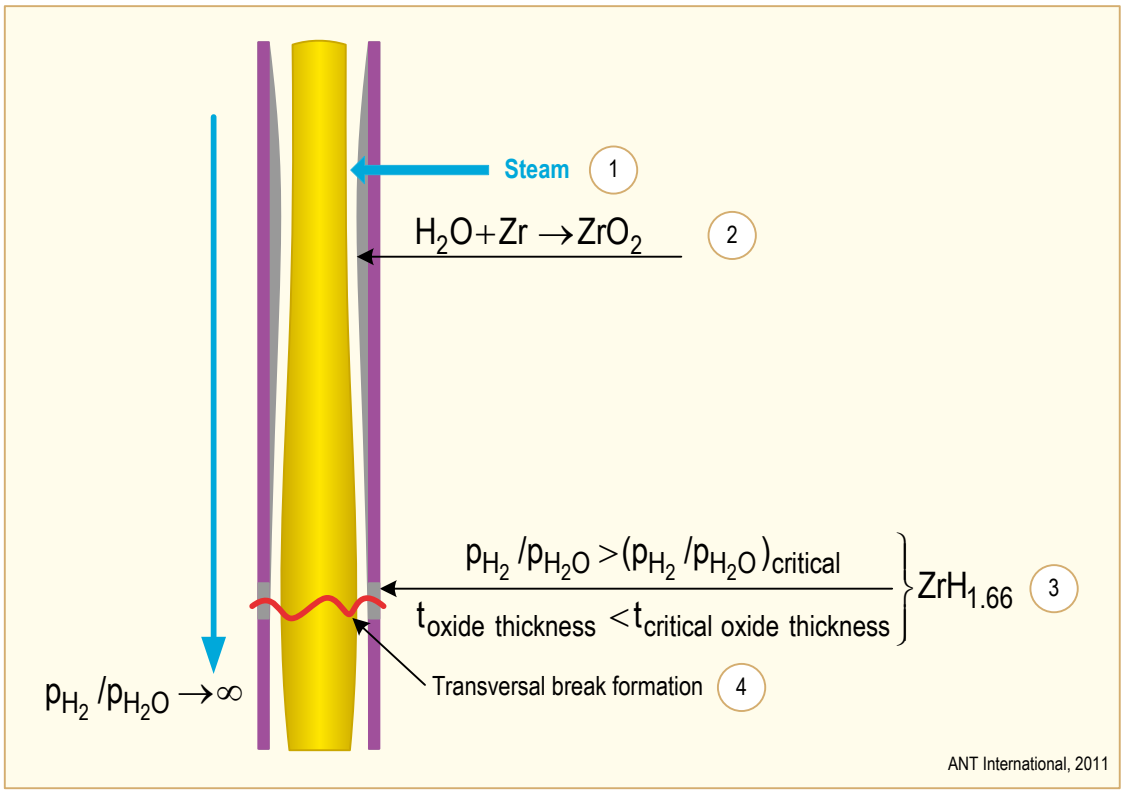


Figure 2-7: Schematics showing the events resulting in transversal break formation. The numbers in the figure relate to the sequence of the different events that may lead to a transversal break.

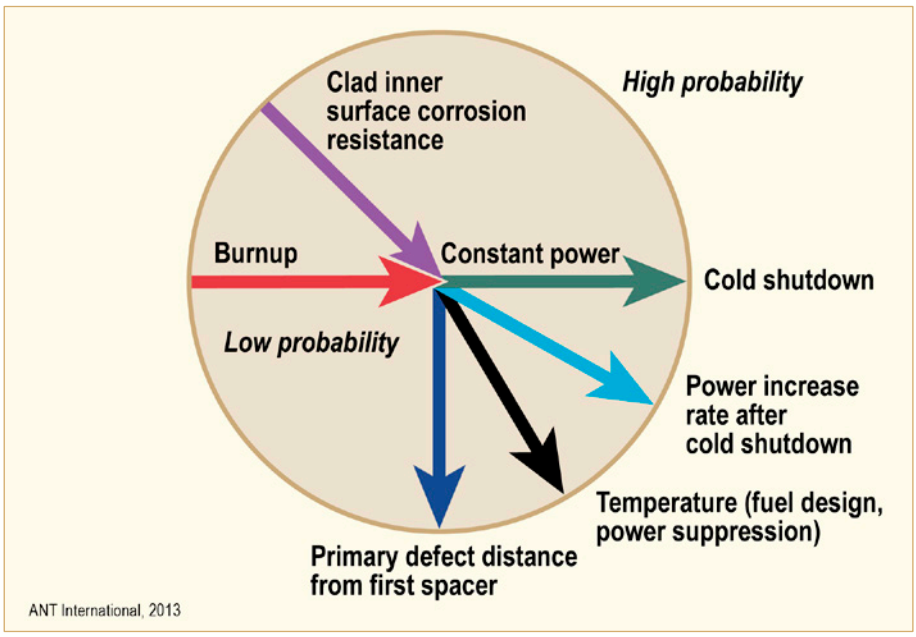


Figure 2-8: Schematics showing the parameters that may impact the transversal break tendency. The centre of the circle represents low probability, while the periphery of the circle represents large risk of getting transversal breaks. Thus, the arrow representing "cladding inner surface corrosion resistance" indicate that increased corrosion resistance will reduce the risk of getting transversal breaks.

### 2.2.2.2 BWR axial split formation

The fuel rod may in principal develop two different types of primary through-wall defects.

The first type A defects consists of sharp through- wall cracks formed during a power ramp either by:

- Propagation of an existing non-through- wall manufacturing defect prior to the ramp.
- Iodine induced SCC mechanisms resulting in PCI cracks.

The second type B defects consist of defects that may be regarded as blunt cracks formed due to corrosion, fretting, etc.

The type A defects are sharp enough to result in a stress intensity factor, K, which during a second ramp may be larger than the critical value for crack propagation provided that the hydrogen solubility in the material is exceeded. This situation may thus result in an axial split without forming any secondary hydriding. It is proposed that the mechanism for crack propagation forming an axial split is a DHC type failure process, see Appendix B, [Strasser et al, 2008] for more details. The lower bounds of the crack velocities are in the range $4 \cdot 10^{-8}$ to $5 \cdot 10^{-7}$ $m \cdot s^{-1}$based on assuming constant growth rates in the time between first detection of the defect and removal of the fuel.

The type B defects are not sharp enough to be able to propagate by itself during a ramp. However, if conditions are such that the ratio of hydrogen to steam partial pressures is larger than a critical value and the clad inner surface oxide thickness is small enough at a certain rod elevation, secondary hydriding may occur at this elevation. Since the specific volume of the hydride is larger than that of the zirconium alloy a large local stress field will build up in and just outside the *hydride blister* and due to that the hydride is brittle, many sharp cracks will form within the *hydride blister* (Figure 2-9). Now as in the case of sharp type A cracks previously discussed, the hydride cracks in the *hydride blister* may propagate during a power ramp by the DHC type mechanism.

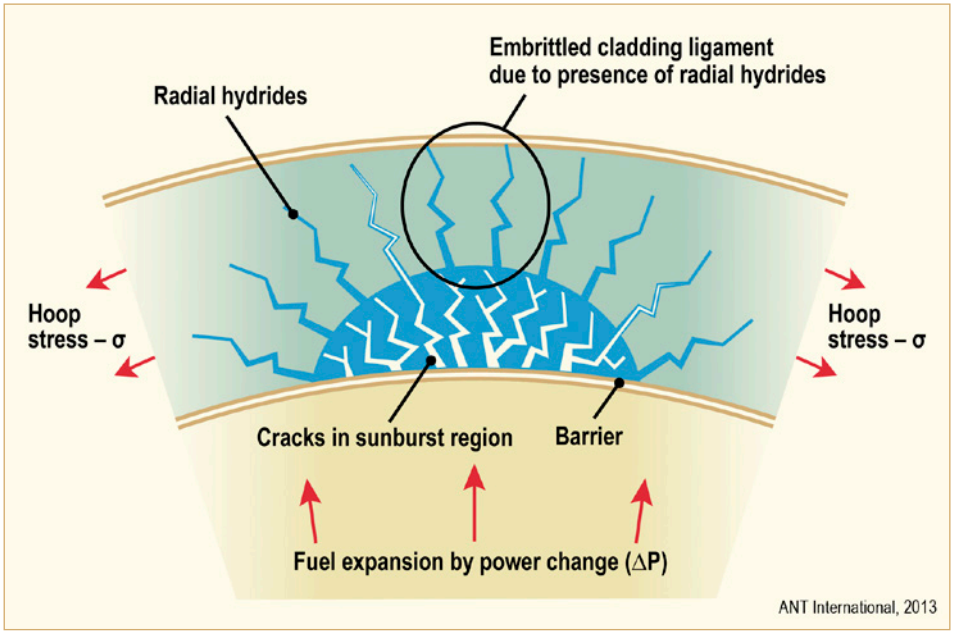


Figure 2-9: Stresses in hydride blisters during power ramping, after [Ozer, 1995].

# 3 Pellet–Cladding-Interaction (PCI) (Ron Adamson and Tahir Mahmood)

**Pellet Cladding Interaction, PCI,** is associated with local power ramps during reactor startup or manoeuvring (e.g., rod adjustments/swaps, load following) (Figure 3-1). When power is increased after some burn-up, the cracked $UO_2$ can expand against the fuel cladding inducing a stress concentration over the cracks. Simultaneously fission products may be released that can cause stress corrosion cracking (SCC) in the cladding, (Figure 3-2). Collectively these processes are called Pellet Clad Interaction - PCI. The crack always starts at the cladding inner surface and progresses towards the outer cladding diameter, usually within minutes of the power increase.

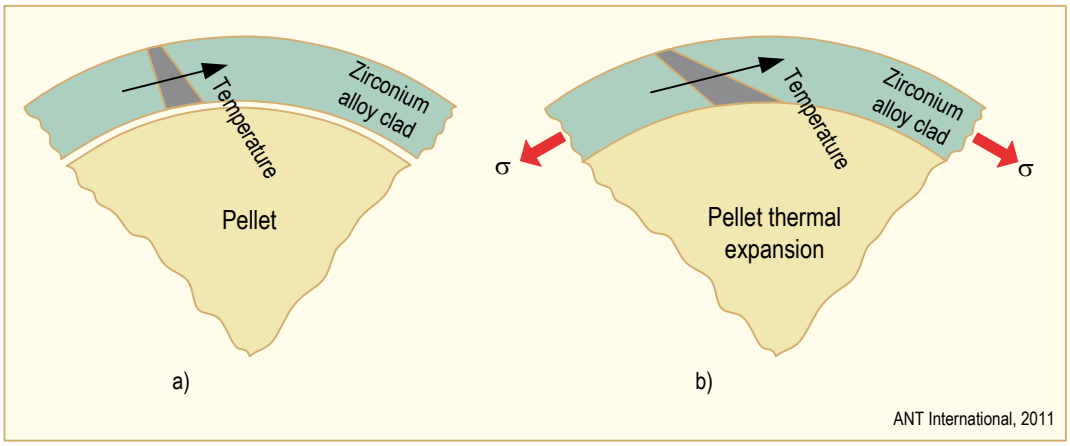


Figure 3-1: Schematic diagram showing the fuel rod condition, (a) before the ramp and, (b) during the ramp.

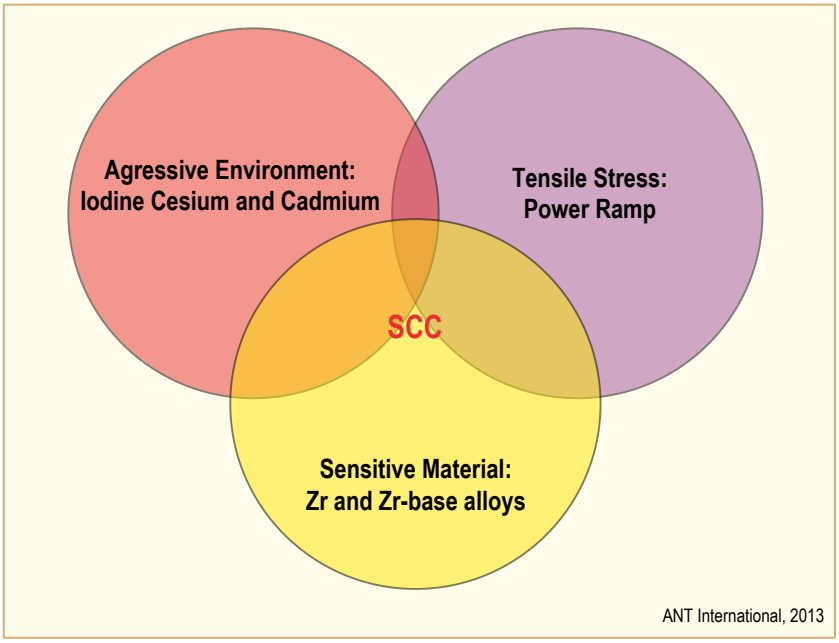


Figure 3-2: Schematic diagram showing the three components involved in SCC.

The typical PCI cracks shown in Figure 3-4 are represented by schematic models in Figure 3-5, Figure 3-6 and Figure 3-7. Features of PCI cracking include:

1) Usually occur after power ramping following significant exposure at low power,

2) On the cladding outside surface the cracks characterized as “short and tight”, visually observed as pinholes or x-marks,

3) Observed plasticity is very small,

4) Metallographic examination usually reveals branching cracks and non-ductile fracture surfaces. In failed fuel the fracture surfaces are often obliterated by post-failure oxidation; however in cases where the crack surface is preserved, transgranular and intergranular fracture features such as in Figure 3-8 are observed. In laboratory testing where texture and testing conditions can be controlled, fracture in iodine can be observed to by cleavage ( or pseudo-cleavage) on basal planes and “fluting” by deformation on pism planes (Figure 3-9), [Aitchison & Cox, 1972].

Details of the cracking process, partially illustrated in Figure 3-3, include:

- Operation of the fuel rod for a time sufficient to generate substantial fission products, 5-10 MWd/Kg U.

- A power increase sufficient to:

  – Raise cladding hoop stress to near the yield stress,

  – Increase in fuel temperature to allow release of fission products to the inner cladding surface. Cracks in the $UO_2$ fuel pellet not only provide localized stress, but may allow a pathway of fission products to the cladding.

- A stress that remains “high” (although decreasing through creep relaxation of the cladding) to allow aggressive fission products to reach and penetrate inner-surface oxide. This process occurs in minutes to tens of minutes.

- Crack initiation on inner surface. Often this initiation is intergranular (particularly at low stress) but can also be transgranular cleavage combined with ductile tearing (fluting) at higher stresses.

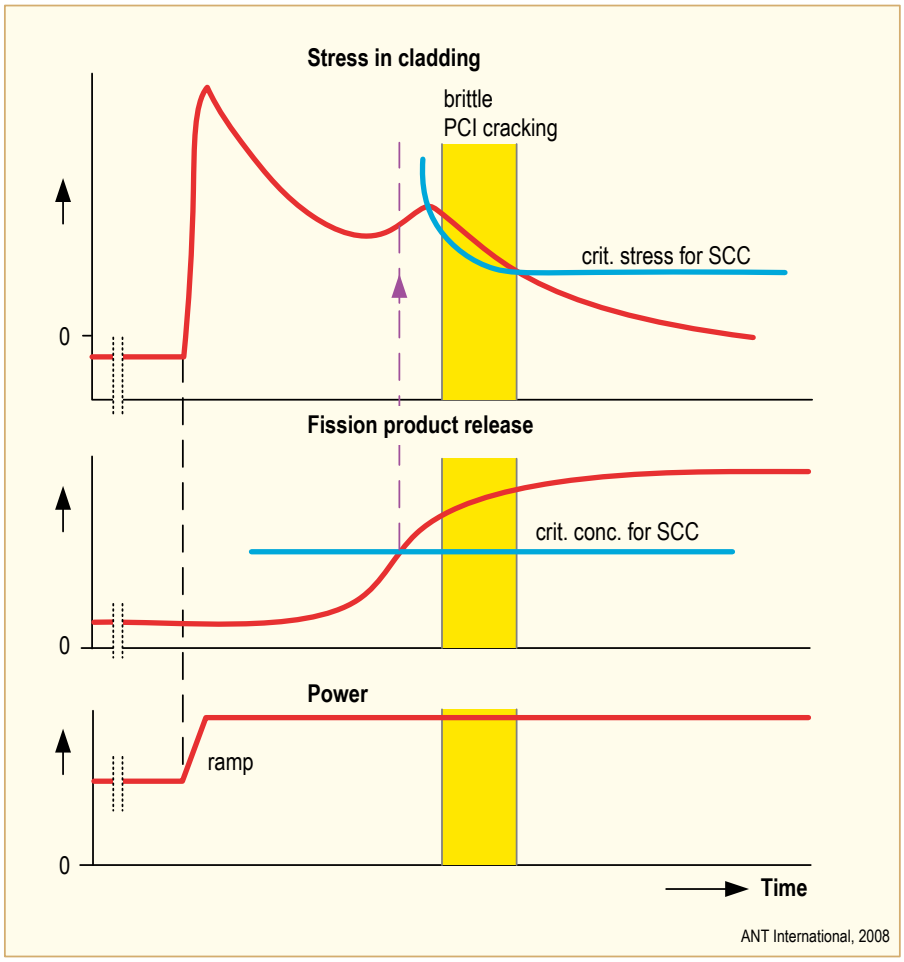


Figure 3-3: Time-dependent model of PCI failure, after [Garzarolli et al, 1978].

- Crack propagation through the wall. Usually only one crack penetrates the wall, but multiple crack initiation can occur:
  - Through-wall penetration occurs quickly, in minutes,
  - The crack size is very small, such that as it reaches the surface it is a fine pinhole, on the order of 25 μm (.001 inch) in "diameter".
- Ending of the stress-corrosion cracking process, as exposure of the crack to steam shuts off the SCC reaction. This stoppage is certainly true for iodine-based reactions, and is less certain for Cd based reactions:
  - Steam flows through the crack and enters the rod interior,
  - The crack surface is oxidized, sometimes to the extent that the pinhole opening is closed by the oxide.
- Crack extension in the axial direction:
  - For relatively low stresses, a short crack, 25-50 μm (1-2 mils), could form. It would look like >---< , a brittle straight crack with ductile shear lips at its ends (the "x-mark"),
  - At higher stresses, further extension in the axial direction might occur. However, since very little hydriding occurs at this location the PCI crack, the primary crack, is usually not the source of long split "secondary cracks".

# 4 Pellet-Cladding Mechanical Interaction (PCMI) (Peter Rudling and Ron Adamson)

## 4.1 Outside-in Cracking (OIC)

### 4.1.1 Introduction

Pellet-cladding mechanical interaction (PCMI), produces cracking that can initiate on the outside surface in a purely mechanical way, helped by hydrides, if the clad tensile stresses during the ramp are large enough. This phenomenon is called outside-inside cracking (OIC).

There are essentially two different PCMI failure modes:

1) If the right conditions exists, a brittle delayed hydride assisted (DHC) cracking mechanism, which is reminiscent of the BWR cladding axial-split phenomena (described in Section 2 of this STR) [Edsinger, 2000], [Lysell et al, 2000], may fail the cladding by crack propagation from the clad OD towards the crack ID. This is a brittle failure mode which means that the cracking surface should be perpendicular to the main clad tensile direction, i.e., in the radial direction. The DHC cracking process is illustrated in Figure 4-1. It is proposed that hydrides form at the crack tip and then fracture, extending the crack. Repetition of this process propagates the crack in the brittle manner observed until the local stress is high enough to cause ductile shear in the residual Zircaloy and the relatively soft zirconium liner. The requirements for DHC to occur are the following:

    a) A clad temperature below a critical value

    b) Hydrides must exist, i.e., the hydrogen content must be larger than the solubility limit

    c) Large enough stress

    d) Long enough time to allow the crack propagation through the cladding thickness

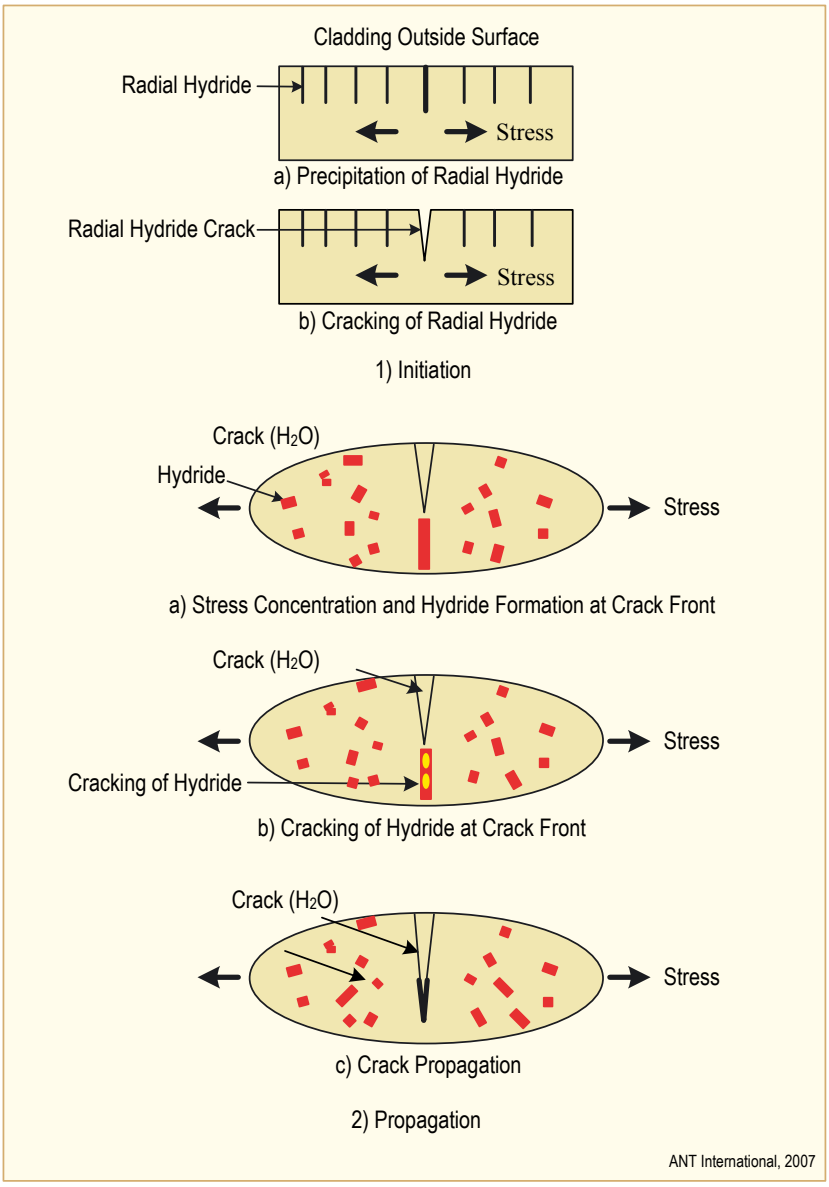


Figure 4-1: Schematic diagram of the crack initiation and DHC propagation process, after [Shimada et al, 2004].

2) If a hydride rim existing at the clad outer surface is thick enough, the cladding may fail by pure ductile mechanical overload of the remaining Zr-alloy ligament that is the only part of the clad cross-section that can support stresses (the oxide and hydride rim are too brittle and will easily crack). The failure is due to plastic shear which means that the sheared surface is oriented 45° towards the circumferential direction.

There have not been any fuel failures in commercial BWRs or PWRs confirmed to be due to PCMI.

### 4.1.2 Ramp testing

In-reactor testing has the best chance to reproduce the conditions present in PCI failures of commercial fuel. For sorting out PCI remedies and mechanisms, the use of test reactors has been useful in the past. Today, there are very few test reactors available for materials testing; e.g., outside of Russia, only Halden and to a lesser extent, Petten and NRU[24] (Atomic Energy of Canada Limited (AECL)) are available for ramp tests. Tests in both commercial and research reactors require related analyses and hot cell examinations, which are complicated and costly but can provide essential input into PCMI understanding.

Many types of ramp tests have been performed, see references[25] – but the most common and most easily described is the "staircase" ramp illustrated in Figure 4-2. Rods for the tests are irradiated in a power reactor at low power to burnups sufficient to generate ample fission products. Rodlets for ramp testing are necessarily short, so it is most convenient to irradiate segmented rods on the

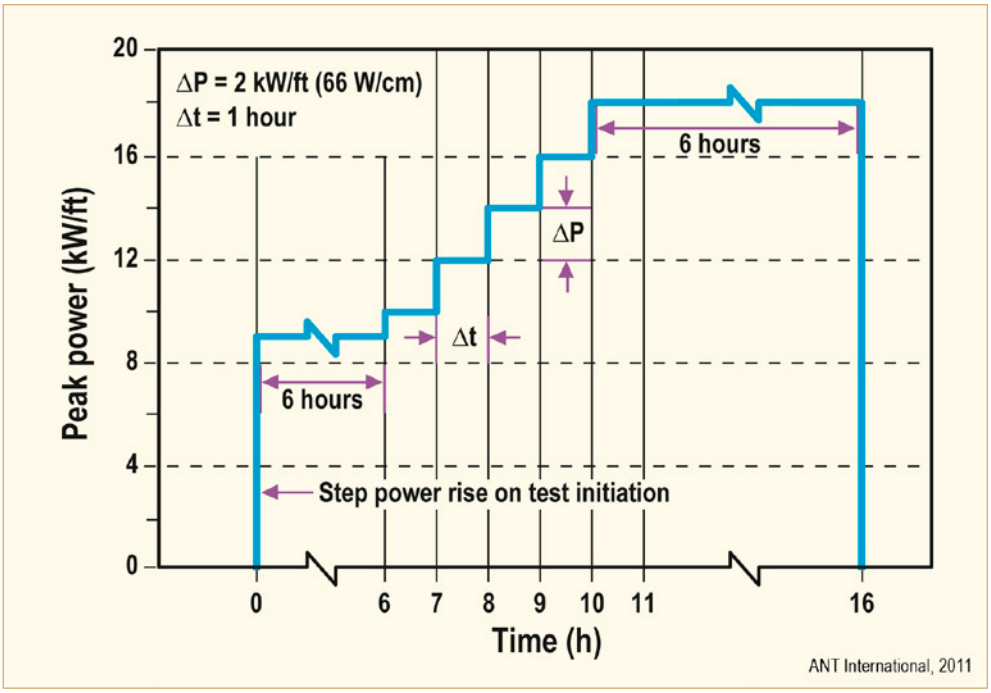


Figure 4-2: Power-ramp sequence illustrating the "staircase" ramp test, after [Davies et al, 1982].

order of a meter long; if full length rods are used they must be refabricated in a hot cell to lengths between a half to one meter. Great care must be taken to prevent contamination of the rod with air, oils, etc. and to prevent pellet fragmentation and relocation during refabrication. In a test reactor, irradiation is conducted for a short time (6 hours in Figure 4-2) at a power similar to the pre-irradiation one in the power reactor. The power is then quickly raised a small amount (about 2 kW/ft (6 kW/m) in Figure 4-2) and held for a short time (1 hour in Figure 4-2).

This sequence is repeated until either the rod fails (detected by monitoring fission products in the coolant, or by dynamic monitoring of the rod length) or a power is reached that is above any power that would be reached in commercial service. The power increments, rates and hold times can be varied to test various hypotheses or fuel conditions (burnup, design, etc.).

[24] Canadian reactor
[25] [Davies et al, 1977, 1984], [Dahlbäck et al, 2005], [Seibold et al, 1997], [Cox, 1990], [Massih et al, 2005], a series of international RAMP projects outlined in [Cox, 1990], p. 271.

# 5 Loss of Coolant Accident (LOCA) (Peter Rudling and Ron Adamson)

## 5.1 Summary Description of the LOCA

The design basis LOCA is a break in a pipe that provides cooling water to the reactor vessel. Analyses are performed for a variety of break sizes and locations to demonstrate that the ECCS can maintain the fuel in a coolable geometry. The limiting break is typically in one of the cold, main coolant pipes of a PWR or one of the intake pipes to the recirculation pump of a BWR.

The LOCA process starts by the decrease and ultimate loss of coolant flow at the same time that the reactor is depressurized (Figure 5-1). The loss of coolant flow decreases heat removal from the fuel, increasing the fuel temperature and causing a significant temperature rise of the cladding. The decrease in system pressure causes an outward pressure differential and a hoop stress in the cladding wall. The result is the plastic deformation, or ballooning of the cladding. Ballooning may also result in fuel relocation[42] that may impact the cladding temperature as well as the Equivalent Cladding Reacted (ECR) in the later phase of LOCA.

**Ballooning and burst –** Ballooning of the fuel rods may result in blockage of the coolant sub-channel that in turn may impact the fuel coolability. If large fuel clad burst strains occur at the same axial elevation, co-planar deformation, in the FA, the coolability may be significantly degraded. Specifically, the clad azimuthal temperature gradient will strongly impact the burst strain. The extent of the ballooning is also dependent on:

- Creep strength of the cladding.
- Stress in the cladding and the corresponding strain rate.
- Temperature and the rate of temperature increase.

Depending on the temperature, the cladding ductility and the rod internal pressure, the cladding will either stay intact or may burst which will allow steam to oxidize the fuel clad inner surface. In addition, some of the hydrogen released by the water/zirconium corrosion reaction inside the burst fuel may be picked up by the cladding resulting in very high local hydrogen concentrations (1000-3000 wtppm H). A fuel cladding with such high hydrogen concentrations will be very brittle even though the cladding is not oxidised at all, i.e. ECR is 0. The fuel clad axial temperature distribution will determine the axial elevation of the ballooned and burst fuel rods in the assembly. The axial and azimuthal fuel clad temperature distribution is a result of the heat transfer mechanisms at the surfaces of the cladding.

[42] Fuel relocation may occur, if during LOCA a section of the fuel rod experiences ballooning, by slumping of fuel fragments from upper location in the ballooned section.

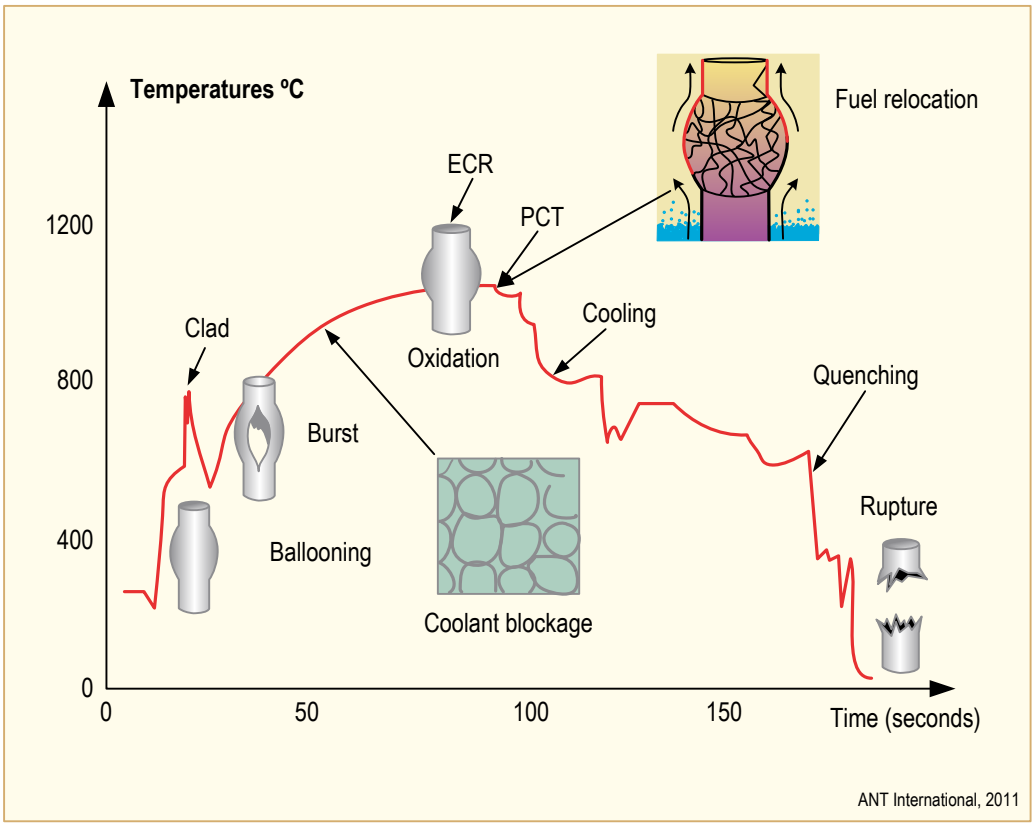


Figure 5-1: Typical LOCA in a PWR.

**LOCA oxidation** – The increasing temperatures and presence of steam will cause the intact cladding to oxidize on the OD and the burst cladding to oxidize on both the OD and ID (two sided oxidation) until the ECCS is activated and the water quenches the cladding. The oxidation process at the high LOCA temperatures will increase the oxygen and hydrogen content in the cladding, reducing its ductility and resistance to rupture. The process and final structure of the cladding after a LOCA cycle is shown on Figure 5-2.

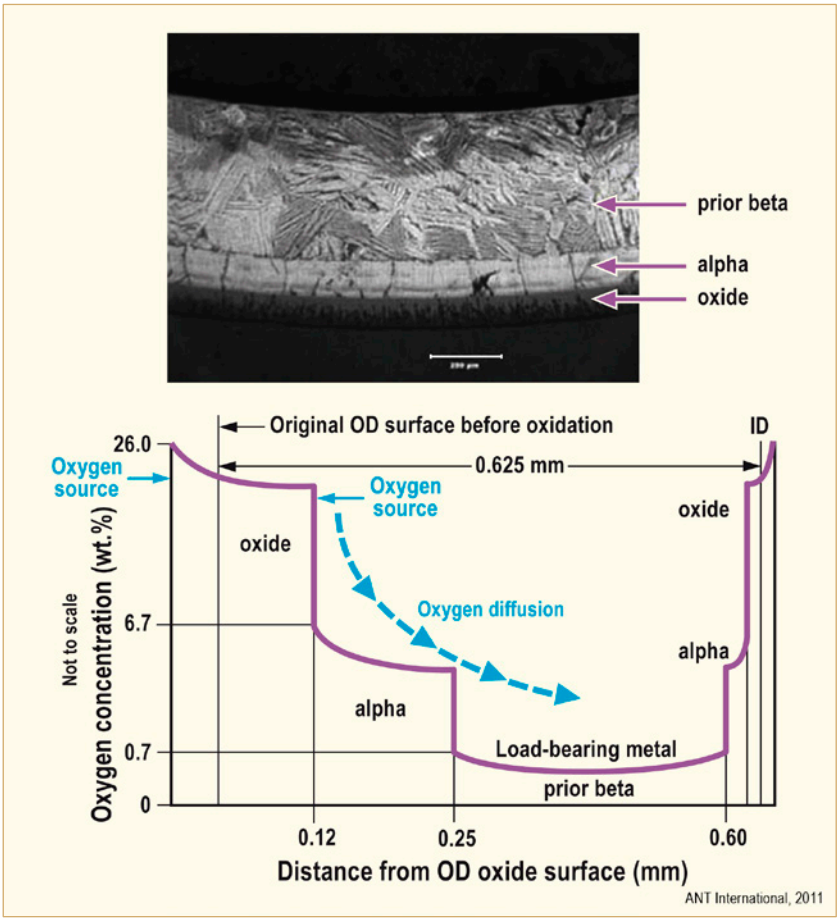


Figure 5-2: Structure of oxidized cladding, after [Meyer, 2005]. (The presence of Nb would result in a similar structure except the boundary between the alpha and the prior beta phase would be more uneven).

- First, the high water and steam temperatures increase their reaction rates with the cladding and increase the conversion of the cladding surface into thicker $ZrO_2$ films.
- As the LOCA temperature passes the levels where α→β transformations start and finish, the resulting structure consists of:
  - The growing $ZrO_2$ layer.
  - A brittle zirconium alloy layer with a very high oxygen content which stabilises the α phase, formed by diffusion of oxygen from the oxide layer.
  - The bulk cladding, which is now in the β phase, has a high solubility for hydrogen; the hydrogen picked up by the cladding from the water-metal reaction increases the solubility of oxygen in the β layer.
- The $ZrO_2$ and oxygen stabilised α layers grow with continued diffusion of oxygen and hydrogen from the water reaction. The increasing amount of oxygen convert some of the β phase to oxygen stabilised α phase with the concurrent shrinkage of the β phase. The remaining β phase cladding wall thickness is transformed to α phase, or "prior β phase", on cooling and is the only structural part of the cladding that can insure its integrity.

# 6 Seismic event (Peter Rudling)

## 6.1 Mechanical design criteria

The mechanical design of the core must meet the safety requirements for seismic accidents or loss of coolant accidents. During such events, large fuel assembly displacements are induced either by the earthquake ground motions transmitted to the reactor core, or by the blowdown-produced pressure forces. The horizontal component of the motion causes lateral fuel assembly distortions and impacts at mixing grid levels between assemblies or with the core plates. In order to prove the reliability of the control rod insertion and of the core cooling, it must be shown that the critical load-bearing fuel components are intact which is;

- The grids for PWRs/VVERs [Collard, 1999 and 2003]
- The fuel outer channel for BWRs

Therefore to assure safe operation following a seismic event, additional criteria are defined. Two levels of ground motion excitation, corresponding to two earthquake levels, are defined for safety-related structures, systems, and components in operating nuclear power plants. Compliance with specified criteria assure that plant safely is maintained following each event.

For the first-level earthquake, the Operating Basis Earthquake (OBE), the load factors and acceptable allowable stresses ensure that the stresses in plant structures remain at least 40 percent below the yield stress of the material for the event.

For the second-level earthquake, the Safe Shutdown Earthquake (SSE), whose vibratory motion is usually twice that of the OBE), the associated load factors and allowable stresses ensure that the stresses in the plant structure and assembly remain close to the yield stress of the specific materials; a small excursion in the inelastic range is allowed when the SSE load is combined with accident loads, usually those associated with a LOCA event.

The following criteria relates to a seismic event:

- OBE-Allow continued safe operation of the FA following an OBE event by establishing that the FA components do not violate their dimensional requirements. This is most simply assured by requiring that the stresses in components remain below the yield stress of the unirradiated components.
- SSE-Ensure safe shutdown of the reactor by maintaining the overall structural integrity of the fuel assemblies, control rod insertability and a coolable geometry within the deformation limits consistent with the ECCS and safety analysis. Requirements to assure safe shutdown are:
  - Fuel rod or assembly fragmentation does not occur due to seismic loads.
  - Control rod insertability is maintained by confirming no or small plastic deformation of components.
    - Adequate static and dynamic crush strength of the spacer assembly (PWR/VVER) and fuel channel (BWR), including requirements for Condition III and IV accidents must be ensured. The grid should maintain the fuel rods in a coolable configuration. The seismic criteria are particularly critical since the PWR/VVER spacers and BWR fuel channels absorb the lateral seismic shocks. This means that the hydrogen content in the Zr alloy spacer (PWR/VVER) and fuel channel (BWR) should be limited.
  - Confirmation that the FA (top and bottom nozzles) maintains engagement with the reactor internals.

To ensure that the criteria above are met, fuel vendors limit the maximum allowable amount of hydrogen in grids (for PWRs/VVERs) and fuel channels (for BWRs) to limit the hydrogen embrittlement effect (Figure 6-1). If the hydrogen content becomes too large in these components, the grids or the fuel channel may fracture due to the seismic load making it difficult to insert the control rods and shut down the reactor.

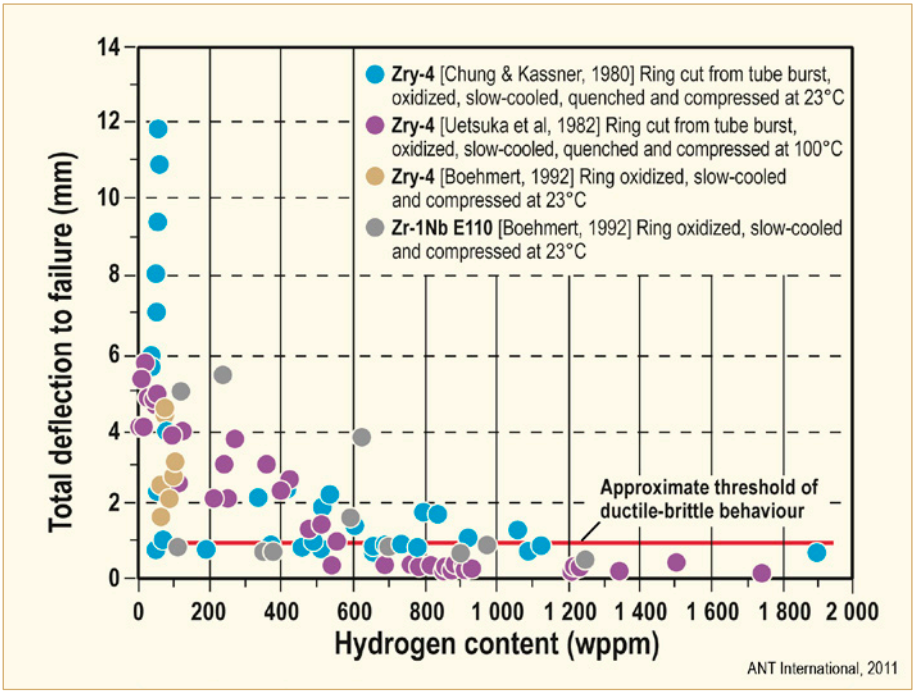


Figure 6-1: Effect of hydrogen on ring compression ductility of unirradiated samples prehydrided before RCT, after [Chung et al, 2001].

## 6.2 Seismic testing

For both BWRs and PWRs/VVERs it must be shown with crush tests that the critical components remain intact during a seismic event.

In the following an example of such testing of PWR bimetallic grids (straps made of Zr-alloy and springs made of Nickel base alloy) grids is provided [Yvon et al, 2005]. Spacer grids irradiated for 1 (11.9 MWd/kgU) and 4 (46.6 MWd/kgU) cycles in a French 900 MW reactor were subjected to crush tests in hot cells at CEA-SACLAY. In addition to the determination of crush limit, special attention was paid to the dummy rod insertion and extraction forces.

Before testing, dummy rods in Zircaloy-4 were introduced in each of the 264 empty cells. These rods were removed after testing to perform visual examinations. The insertion and extraction of the rods within the grid are measured on 25 cells evenly distributed within the grid. These measurements are performed on each individual rod through a KISTLER force sensor at a rate of 1 mm/s.

The buckling tests involve laterally compressing a grid between two tables, one upper fixed one, connected to the force sensor, the other “lower” mobile and integral with the hydraulic jack. Figure 6-2 represents the set-up used. A three-zone furnace is used to run the buckling tests at 325 + 10°C. Use is made of three calibrated thermocouples, arranged on the furnace wall for controlling the temperature in the three zones. The temperature of the grid equipped with the rods is monitored by three calibrated thermocouples, arranged in the grid as shown in Figure 6-3.

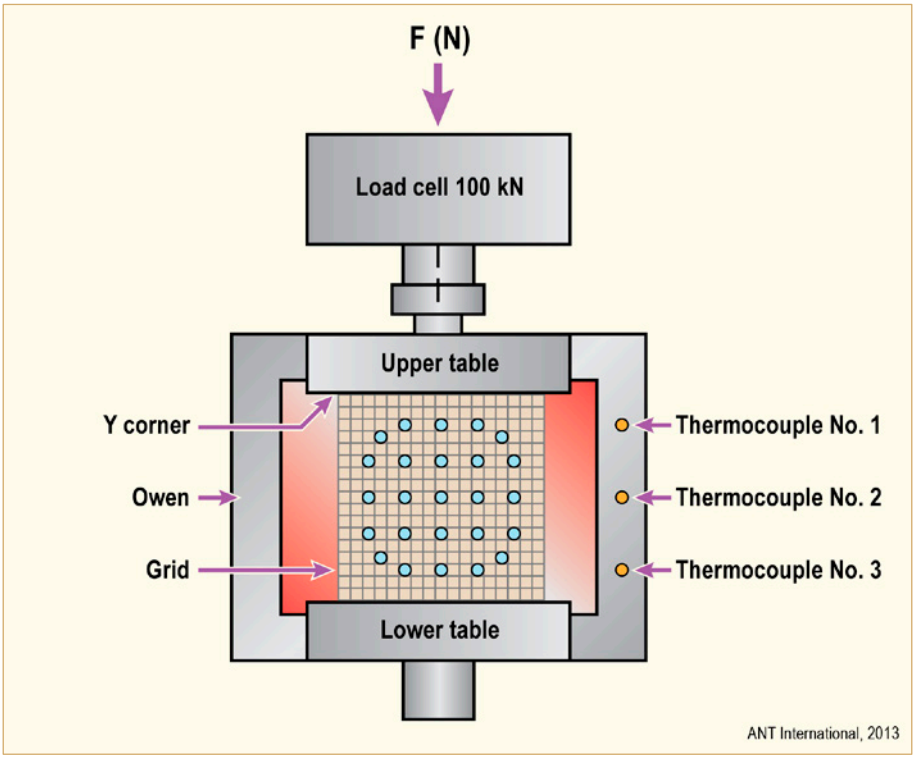


Figure 6-2: Grid compression test setup.

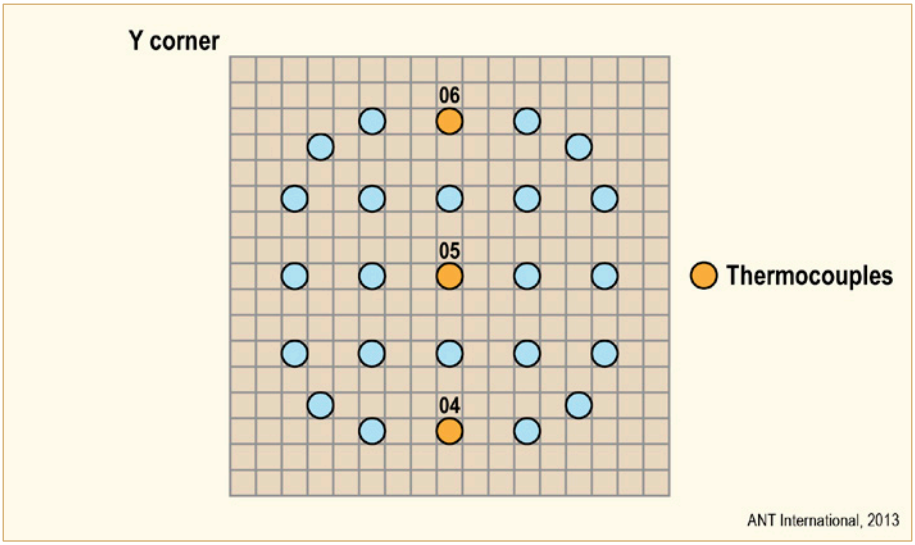


Figure 6-3: Location of thermocouples within the grid, view from the top.

To run the tests, an INSTRON 100 kN tension-compression hydraulic machine and a PYROX furnace, were used. All the tests were performed in displacement control mode at a rate of 40 mm/s.

# 7 Dry storage (Tahir Mahmood)

ANT International is preparing a dry storage handbook, which is also scheduled for publication in 2013, in parallel to this STR. The handbook covers issues related to spent nuclear fuel and dry storage in greater detail than is possible in this STR. Therefore, we are deferring comments on testing techniques to the upcoming handbook. The reader is directed to this handbook for details [Franklin et al, 2013]. A brief introduction is presented below.

In the late 1970s and early 1980s, the need for alternative storage began to grow when pools at many nuclear reactors began to fill up with stored spent fuel. Utilities began looking at options such as dry cask storage for increasing spent fuel storage capacity. Dry cask storage allows spent fuel that has already been cooled in the spent fuel pool for at least one year to be surrounded by inert gas inside a container called a cask. The casks are typically steel cylinders that are either welded or bolted closed. The steel cylinder provides a leak-tight confinement of the spent fuel. Each cylinder is surrounded by additional steel, concrete, or other material to provide radiation shielding to workers and members of the public. Some of the cask designs can be used for both storage and transportation.

There are various dry storage cask system designs. In some designs, typically identified as canister storage systems, steel cylinders containing the fuel are placed vertically in a concrete vault; other designs orient the cylinders horizontally. The concrete vaults provide the radiation shielding. In other designs, which are typically oriented vertically on a concrete pad at a dry cask storage site, metal containers (casks) are used either with or without metal and concrete outer cylinders (overpacks) for radiation shielding. Typical dry cask storage systems are shown in Figure 7-1. Spent fuel is currently stored in dry cask systems at a growing number of power plant or storage sites in all but a few nuclear countries.

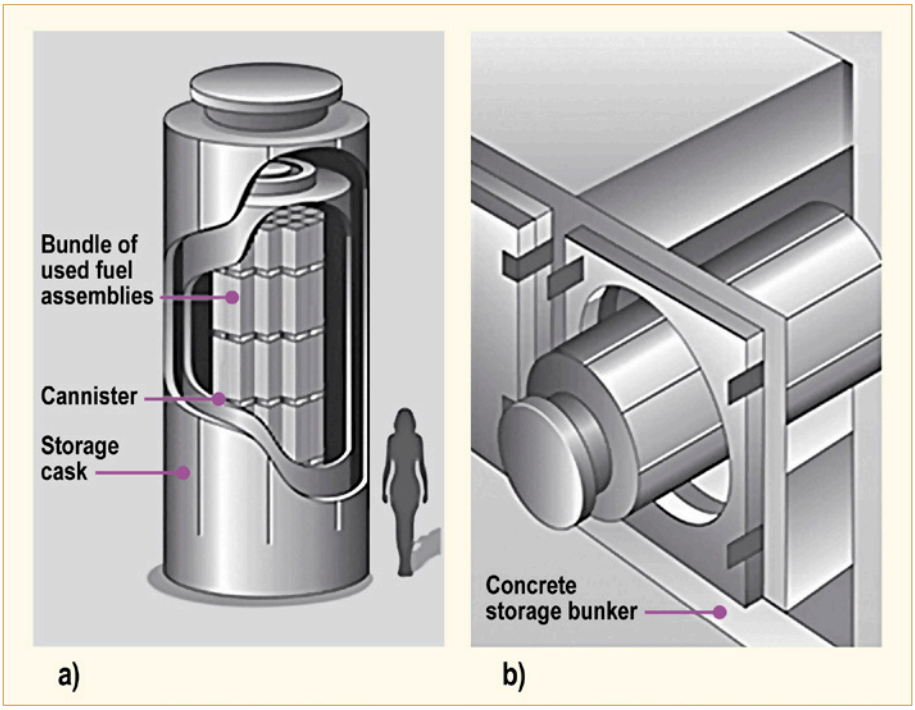


Figure 7-1: Some canisters are designed to be placed vertically in robust above-ground concrete or steel structures (a) and some canisters are designed to be stored horizontally in above-ground concrete bunkers, each of which is about the size of a one-car garage. [From USNRC web page http://www.nrc.gov/waste/spent-fuel-storage/diagram-typical-dry-cask-system.html].

# 8 Creep Rupture (Kit Coleman)

## 8.1 Phenomenology

Components may deform by creep when loaded in tension for long times. The time dependence of creep is shown in Figure 8-1. Three main stages include:

- Stage I or primary creep where the initial high rate of deformation gradually diminishes towards
- Stage II or secondary or steady state creep where the rate of deformation is approximately constant. This deformation rate is also called the minimum creep rate (MCR) when it is followed by
- Stage III or tertiary creep where the deformation rate starts to increase and leads to rupture.

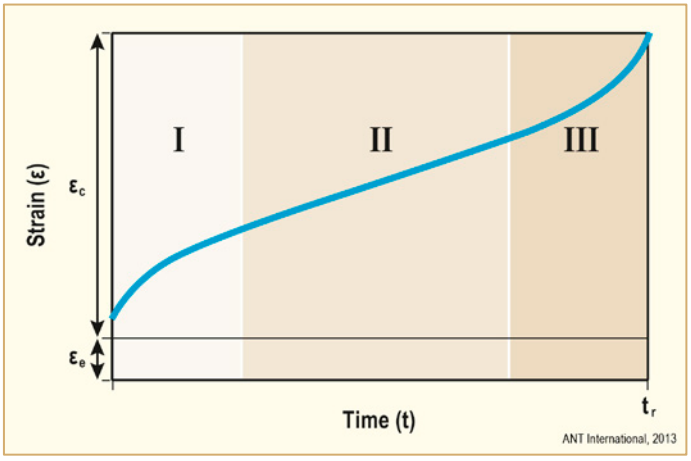


Figure 8-1: Typical creep curve showing initial loading strain, εe, mostly elastic, followed by various stages of creep strain: stage I called primary creep, stage II called secondary creep or minimum creep rate (MCR), stage III called tertiary creep leading to rupture at time $t_r$.

Low creep strains and their consequences for components' viability are discussed in Volume 1, Section 6. Now the residual capacity for strain and the potential for creep rupture are evaluated during normal reactor operation. The operation of a pressure tube is used as an example because it is exposed to tensile stresses, temperatures around 300°C and a neutron flux of about $3x10^{17}$ n/m$^2$ throughout its lifetime of up to 30 years.

Fracture by creep is caused by the onset of the inability of the specimen or component to carry the applied load. If no external chemical reaction interferes, for example, oxidation, two categories of how the load-bearing cross-section is lost are:

1) In the absence of cavities, when volume is conserved, the cross-section simply decreases as the specimen deforms in response to the applied stress.

2) If cavities form, they also contribute to the loss in cross-section. The area, $A_1$, of a cross-section containing a uniform array of spherical cavities with radius r and spacing λ is related to an area $A_0$ that is cavity-free through:

Eq. 8-1: $$A_1 = A_0 [1-\pi(r/\lambda)^2]$$

When r/λ is 0.05 the area loss is <1%, it increases to 10% when r/λ is 0.18 and reaches 50% when r/λ approaches 0.4.

The consequence of the concomitant increase in tensile stress, σ, depends on how the rate of plastic flow, $\dot{\varepsilon}$ , changes with stress. With a simple power law, $\dot{\varepsilon} \propto \sigma^n$, an increase in creep rate is expected. Rupture follows either when the cross-section is so reduced that the UTS is exceeded or the ratio of the initial creep rate to the final creep rate, $\dot{\varepsilon}_r$ goes to infinity. If the initial creep rate is represented by MCR, then the time to rupture, $t_r$, was derived by [Burton, 1982] to be:

Eq. 8-2: $$(MCR).n.t_r = 1$$

when $\dot{\varepsilon}_r/MCR \rightarrow \infty$.

Earlier, [Monkman & Grant, 1956] plotted creep rupture data of many materials and found that:

Eq. 8-3: $$\log t_r + \zeta.\log (MCR) = \psi$$

when $\zeta = 1$, Eq. 8-3 becomes:

Eq. 8-4: $$(MCR).t_r = \text{constant}$$

having the same form as Eq. 8-2. The constant in Eq. 8-4 has the units of strain and has a value of 1/n in uniaxial loading and 1/2n with internal pressurization of a tube.

When values of $t_r$ and MCR for zirconium alloys are plotted as indicated (Figure 8-2), $\zeta \approx 1$. These results are from a wide array of materials and test conditions (Table 8-1), [Coleman, 1972], [Ibrahim & Coleman, 1973], [Clay & Redding, 1976], [Burton, 1983a], [Limon & Lehmann, 2004]. The results suggest that the same phenomenology applies to different alloys, both α- and β-phases, different loading conditions and whether the material is irradiated or not, and therefore can be applied to several practical situations.

Table 8-1: Correlation between minimum creep rate and time to rupture for zirconium alloys.

| Material | Test details | Test temperatures (°C) | Stress (MPa) | χ | MCR x tr | Reference |
|---|---|---|---|---|---|---|
| CW Zircaloy-2, pressure tube | Uniaxial specimen, axial direction | 350 | 290 - 355 | 1.018 | 0.045 | [Coleman, 1972] |
| CW Zircaloy-2, pressure tube | Uniaxial specimen, axial direction | 300 - 450 | 140 - 380 | 1.025 | 0.052 | [Ibrahim & Coleman, 1973] |
| CW Zr-2.5Nb, pressure tube | Uniaxial specimen, axial direction | 300 - 450 | 140 - 570 | 0.991 | 0.064 | [Ibrahim & Coleman, 1973] |
| CWSR & RX Zircaloy-2 fuel cladding | Tube specimen, internally pressurized | 700 - 800 | 13 - 66 | 0.994 | 0.131 | [Clay & Redding, 1976] |
| RX Zircaloy-4 strip; α-phase | Uniaxial specimen | 700 - 800 | 10 - 50 | 1.012 | 0.287 | [Burton, 1983a] |
| Zircaloy-4 wire; β-phase, bamboo structure | Uniaxial specimen | 1050 - 1150 | 0.5 - 1.7 | 1.008 | 0.118 | [Burton, 1983a] |
| CWSR Zircaloy-4 cladding | Tube specimens, internal pressure | 350 - 470 | 100 - 550 | 0.824 | 0.065 | [Limon & Lehmann, 2004] |
| CWSR Zircaloy-4 cladding irradiated between 0.4 to 9.5 x$10^{25}$ n/$m^2$ | Tube specimens, internal pressure | 350 - 470 | 100 - 550 | 1.164 | 0.043 | [Limon & Lehmann, 2004] |

ANT International, 2013

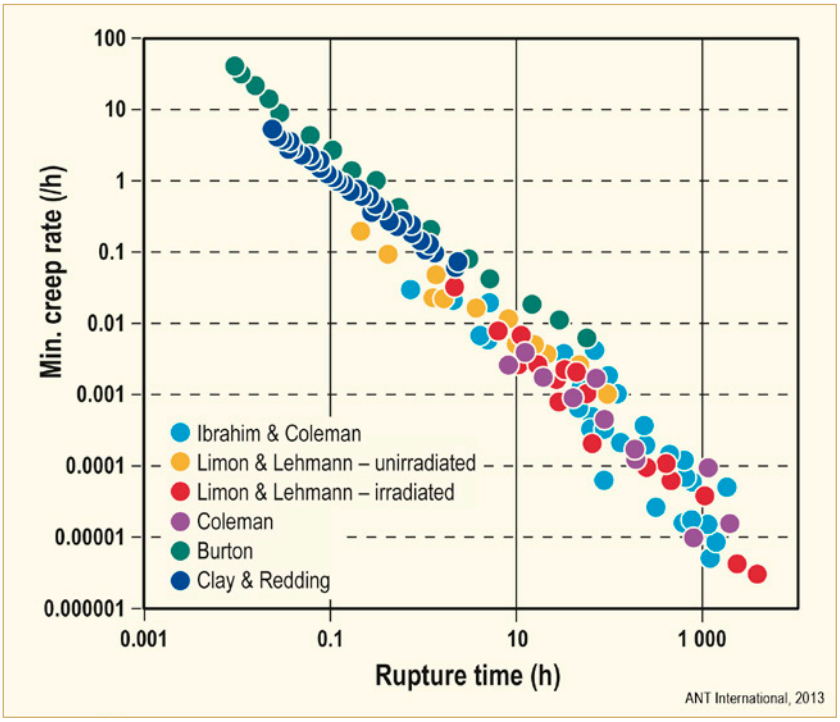


Figure 8-2: Relationship between minimum creep rate and rupture time in zirconium alloys, after [Coleman, 1972], [Ibrahim & Coleman, 1973], [Clay & Redding, 1976], [Burton, 1983a], [Limon & Lehmann, 2004].

In many materials, cavities may be formed throughout the component or specimen during creep [Evans, 1984]. These processes require diffusion. As a consequence, the elongation at rupture decreases as the time to rupture increases; Figure 8-3 shows the behaviour of phosphorus-doped oxygen-free copper tested over a range of temperatures 200 to 600°C [Andersson-Östling & Sandström, 2009]; at each temperature the creep ductility declines as the rupture time increases. In out-reactor tests on zirconium alloys, the same pattern is not observed as elongation tends to increases with rupture time [Watkins & Wood, 1969], [Ibrahim & Coleman, 1973], [Limon & Lehmann, 2004], for example, in tests on material from fuel cladding (Figure 8-4a), and pressure tubes (Figure 8-4b), at temperatures between 300 and 400°C. Zirconium is very resistant to forming cavities from deformation or voids from irradiation [Burton, 1983b], [Yoo, 1974]. Metallography and density measurements after creep testing of Zircaloy-2 indicate that cavities only form in the elevated hydrostatic tensile stress of a neck in uniaxial creep tests leading to ductile fracture [Coleman, 1972], similar to the behaviour in a tensile test [Gaillac et al, 2011].

# 9 References

10 CFR Part 50 Appendix A, *General Design Criteria for Nuclear Power Plant*s, US, Government Printing Office, Washington, 1990.

10 CFR Part 100.11, *Determination of Exclusion Area, Low Population Zone, and Population Centre Distance*, US Government Printing Office, Washington, 1990.

10 CFR Part 100, NRC, Standard Review Plan, NUREG-0800, USNRC, 1995.

Abriata J. P. Garces J. and Versaci R., Bull. Alloy Phase Diagrams 7(2), pp. 116-124, 1986.

Adamson R. B., *Effect of Texture on Stress Corrosion Cracking of Irradiated Zircaloy in Iodine*, J. Nucl. Mat. 82, pp. 363, 1980.

Adamson R. B. and Bell W. L., *Effects of Neutron Irradiation and Oxygen Content on the Microstructure and Mechanical Properties of Zircaloy*, Microstructure and Mechanical Behaviour of Materials, Proceedings: Int'l Symposiums, Xian, China, October, 1985, EMAS, pp. 237-246, Warley, UK, 1986.

Adamson R. B., Wisner, S. B., Tucker, R. P. and Rand. R. A., *Failure Strain for Irradiated Zircaloy Based on Subsized Specimen Testing and Analysis*, The Use of Small-Scale Specimens for Testing Irradiated Material, ASTM STP 888, W. R. Corwin and G. E. Lucas, Eds., American Society for Testing and Materials, 171-185, Philadelphia, 1986.

Adamson R. B., *Effects of Neutron Irradiation on Microstructure and Properties of Zircaloy*, Zirconium in the Nuclear Industry; Twelfth International Symposium, ASTM STP 1354, pp. 15-31, West Conshohocken, PA, 2000.

Adamson R., Cox B., Davies J., Garzarolli F., Rudling P. and Vaidyanathan S., *Pellet-Cladding Interaction (PCI and PCMI)*, ZIRAT11/IZNA6, Special Topics Report, ANT International, Mölnlycke, Sweden, 2006/2007.

Adamson R. B, Garzarolli F. and Patterson C., *In-Reactor Creep of Zirconium Alloys*, ZIRAT14/IZNA9 Special Topical Report, ANT International, Mölnlycke, Sweden, 2009.

Adamson R. B, Garzarolli F., Patterson C., Rudling P. Strasser A. and Coleman K., *ZIRAT15/IZNA10 Annual Report*, ANT International, Mölnlycke, Sweden, 2010.

Adroguer B., Hueber C., and Trotabas M., *Behaviour of PWR Fuel in LOCA Conditions, PHEBUS Test 215 P*, presented at OECD-NEA-CSNI/IAEA Specialists' Meeting on Water Reactor Fuel Safety and Fission Product Release in Off-Normal and Accident Conditions, Ris0 National Laboratory, Denmark, May 1983.

Agee L. J., Dias A. F., Eisenhart L. D. and Engel R. E., *Realistic scoping study of reactivity insertion accidents for a typical PWR and BWR core*, Proc. CSNI specialist meeting on transient behaviour of high burnup fuel, pp 291-304, Cadarache, France, September 12-14, 1995.

Aitchison I. and Cox B., *Interpretation of Fractographs of SCC in Hexagonal Metals*, Corrosion, Vol. 28, pp. 83 – 87, 1972.

Alvarez-Holston A-M. et al, *Studies of Hydrogen assisted Failures Initiating at the Cladding Outer Surface of High Burn-up Fuel using a Modified Ring-Tensile Technique*, Proc. 2007 Int. LWR Fuel Performance Meeting, pp. 1080, San Francisco, CA, 2007.

Alvarez-Holston A-M., Grigoriev V., Lysell G., Källström R., Johansson B., Hallstadius L., Zhou G., Arimescu I. and Lloret M., *A Combined Approach to Predict the Sensitivity of Fuel Cladding to Hydrogen-Induced Failures during Power Ramps*, Proceedings of 2010 LWR Fuel Performance/TopFuel/WRFPM, Orlando, Florida, USA, September 26-29, 2010.

Andersson T. and Wilson A., *Ductility of Zircaloy canning tubes in relation to stress ratio in biaxial testing* In: Zirconium in the nuclear industry; 4th international symposium, J. H. Schemel and T. P. Papazoglou, Editors, American Society for Testing and Materials, ASTM STP-681, pp. 60-71, 1979.

Andersson-Östling H. C. M. and Sandström R., *Survey of creep properties of copper intended for nuclear waste disposal*, Swedish Nuclear Fuel and Waste Management Co., Technical Report TR-09-32, 2009.

Anghel C., Alvarez Holston A. M., Lysell G., Karlsson S., Jakobsson R., Sund E., Mahmood S. T., *An Out-of-Pile Method to Investigate Iodine-induced SCC of Irradiated Cladding*, Proceedings of the Top Fuel conference, Paris, France, 2009.

Anghel C., Alvarez Holston A. M., Lysell G., Karlsson S., Jakobsson R., Flygare J., Mahmood S. T., Boulch D. L., Arimescu I., *Experimental and Finite Element Modelling Parametric Study for Iodine-Induced Stress Corrosion Cracking of Irradiated Cladding*, Proceedings of the ANS/Top Fuel conference, Orlando, Florida, USA, 2010.

Armijo J. S., *Performance of Failed BWR Fuel*, Proceeding from Light-Water-Reactor-Fuel-Performance, pp. 410-422, West Palm Beach, FL, April 17-21, 1994.

Arséne S. and Bai J. B., *A new approach to measuring transverse properties of structural tubing by a ring tes*t, Laboratory MSS/MAT, Ecole Centrale Paris, CNRS URA 850, 92295 Chatenay Malabry Cedex, France 1996.

ASME, *Rules for Construction of Nuclear Power Plants Components*, ASME Boiler and Pressure Vessel Code, Section III, 2010.

Bahurmuz A. A., Muir I. J. and Urbanic V. F., *Predicting oxidation and deuterium ingress for Zr-2.5Nb CANDU pressure tubes,* ASTM STP 1467, pp. 547-562, (2005). Or J. ASTL international, Vol. 2, n°5, JAI 12342, May 2005.

Bates D. W., Koss D. A., Motta A. T. and Majumdar S., *Influence of Specimen Design on the Deformation and Fracture of Zircaloy Cladding*, Proceedings of the ANS Int. Topical Mtg. on LWR Fuel Performance, American Nuclear Society, pp. 1201-1210, Park City, UT, 2000.

Bernaudat C. and Pupiers P., *A new analytical approach to study the rod ejection accident in PWRs*, Reactor Fuel Performance Meeting, paper no. 1127-Trace no. 5, Kyoto, 2005.

Bibilashvili Y. K. et al, *WWER-1000 type fuel assembly tests on electroheated facilities in LOCA simulating conditions*, IAEA Technical Committee Meeting on Fuel behaviour under transient and LOCA conditions, pp. 169-185, Halden, Norway, 2001.

Bibilashvili Yu. K., Sokolov N. B., Salatov A. V., Tonkov V. Yu., Fedotov P. V., Andreeva-Andrievskaya L. N., Deniskin V. P., Nalivaev V. I., Parshin N. Ya., Afanasyev P. G., Konstantinov V. S., Semishkin V. P. and Shumski A. M., *WWER-1000 Type Fuel Assembly Tests on Electroheated Facilities In LOCA Simulating Conditions*, IAEA-TECDOC-1320, 2002.

Bickel G. A., Private communication, 2013.

Billone M. C., Burtseva T. A. and Einziger R. E., *Ductile-to-brittle transition temperature for high-burnup cladding alloys exposed to simulated drying-storage conditions,* Journal of Nuclear Materials 433, pp. 431–448, 2013.

Blomberg G., *Results of recent Hot Cell examinations of failed fuel at Studsvik, Sweden*, 35th International Utility Nuclear Fuel Performance Conference, 2006.

Bouffioux P. and Legras L., *Effect of hydriding on the residual cold work recovery and creep of Zircaloy 4 cladding tubes*, Proc: ANS conference on fuel performance, Park City, USA, 2000.

Bouffioux P. and Rupa N., *Impact of Hydrogen on Plasticity and Creep of Unirradiated Zry-4 Cladding Tubes*, Zirconium in the Nuclear Industry: Twelfth International Symposium, ASTM STP 1354, Sabol G. and Moan G., Eds., American Society for Testing and Materials, pp. 399-422, West Conshohocken, PA, 2000.

Brachet J-C., Pelchat J., Hamon D., Maury R., Jacques P. and Mardon J-P., *Mechanical Behaviour at Room Temperature and Metallurgical Study of Low-Tin Zy-4 and M5TM (Zr-NbO) Alloys after Oxidation at 1100°C and Quenching*, Proceeding of IAEA TCM on Fuel behaviour under transient and LOCA conditions, IAEA-TECDOC-1320, Halden, Sept. 10-14, 2001.

Brachet J. C., Portier L., Forgeron T., Hivroz J., Hamon D., Guilbert T., Bredel T., Yvon P., Mardon J–P. and, Jaques P., *Influence of hydrogen content on the α/β phase transformation temperatures and on the thermal-mechanical behaviour of Zry-4, M4 and M5 (ZrNbO) alloys during the first phase of LOCA transient*, Zirconium in the Nuclear Industry: Thirteenth International Symposium, ASTM STP 1423, G. D. Moan and P. Rudling, Eds., ASTM International, West Conshohocken, PA, 2002.

Brachet J. et al, *Hydrogen Content, Pre-Oxidation and Cooling Scenario Influences on Post-Quench Mechanical Properties of Zy-4 and M5 Alloys in LOCA Conditions – Relationship with the Post-Quench Microstructure*, 15th Int. Conf. on Zirconium in the Nuclear Industry, ASTM, Sun River, Oregon, June, 2007.

Burton B., *The upper limit to the creep life of solids under a tensile force*, J. Mat. Sci., 17, 2441-2448, 1982.

Burton B., *Creep fracture processes in Zircaloy*, J. Nucl. Mater., 113, 172-178, 1983a.

Burton B., *A criterion for predicting creep fracture mechanisms*, Res Mech., 8, 235-259, 1983b.

Busby C. C., Tucker R. P., and McCauley J. E., J. Nucl. Mat. 55, pp. 64, 1975; and in Bettis Atomic Power Laboratory Report WAPD-TM1149, 1974.

Carassou S. et al, *Ductility and Failure Behaviour of both Unirradiated and Irradiated Zircaloy-4 Cladding Using Plane Strain Tensile Specimens*, OECD/NEA Workshop, Nuclear Fuel Behaviour during RIA, Paris, Sept. 2009.

Cazalis B., Bernaudat C., Yvon P., Desquines J., Poussard C. and Averty X., *The Prometra Program: A Reliable Material Database for Highly Irradiated Zircaloy-4™ and M5™ Fuel Claddings*, Proc. 18th International Conference on Structural Mechanics in Reactor Technology, SMiRT 18-C02-1, Beijing, China, August 7-12, 2005.

Chapin D. L., Wikmark G., Maury C., Thérache B., Gutiérrez M. Q. and Muñoz-Reja Ruiz C., *Optimized ZIRLO Qualification Program for EdF Reactors*, Proceedings of Top Fuel 2009, pp. 2040, Paris, France, September 6-10, 2009

Chapman R. H., *Multi-rod burst test program: progress report, July-December 1977*. ORNL/NUREG/TM-200, June 1978.

Cheadle B. A., Ells C. E. and van der Kuur, J., *Plastic Instability in Irradiated Zr-Sn and Zr-Nb Alloys*, Zirconium in Nuclear Applications, ASTM STP 551, American Society for Testing and Materials, 370-384, 1974.

Cheadle B. A., Coleman C. E., Ambler J. F. R., *Prevention of delayed hydride cracking in zirconium alloys*, ASTM STP 939, Zirconium in the Nuclear Industry – Seventh International Symposium, R. B. Adamson and L. F. P. Van Swam, Eds., American Society for Testing and Materials, 224-240, Philadelphia, PA., 1987.

# Nomenclature

| | |
|---|---|
| AECL | Atomic Energy of Canada Limited |
| ALARA | As Low As Reasonably Achievable |
| ANF | Advanced Nuclar Fuel |
| ANL | Argonne National Laboratory |
| AOO | Anticipated Operational Occurrences |
| ASME | American Society of Mechanical Engineers |
| ATR | Advanced Test Reactor |
| BL | Burst Lenght |
| BOL | Beginning of Life |
| BT | Burst Temperature |
| BW | Burst Width |
| BWR | Boiling Water Reactor |
| CAC | Corrosion Assisted Cracking |
| CANDU | Canadian Deuterium Uranium |
| CEA | Commissariat à l'Energie Atomique |
| CEB | Closed End Burst |
| CERT | Constant Extension Rate Test |
| CFR | Code of Federal Regulations |
| CHC | Corrosion Hydrogen Cracking |
| CHF | Critical Heat Flux |
| CPR | Critical Power Ratio |
| CRB | Control Rod Blade |
| CRDA | Control Rod Drop Accident |
| CREA | Control Rod Ejection Accident |
| CRUD | Chalk River Unidentified Deposits |
| CSED | Critical Strain Energy Density |
| CT | Compact Tension |
| CW | Cold Work |
| CZP | Cold Zero Power |
| DBA | Design Base Accident |
| DBTT | Ductile-to-Brittle Transition Temperature |
| DHC | Delayed Hydride Cracking |
| DNB | Departure from Nucleate Boiling |
| DNBR | Departure from Nucleate Boiling Ratio |
| EBT | Equal biaxial tension |
| ECCS | Emergency Core Cooling System |
| ECR | Equivalent Clad Reacted |
| EDC | Expansion due to Compression |
| EDM | Electric Discharge Machnining |
| EPRI | Electric Power Research Institute |
| ESCP | Extended Storage Collaboration Program |
| ETR | Engineering Test Reactor |
| FA | Fuel Assembly |
| FALCON | Fuel Analysis and Licensing Code |
| FE | Finite Element |
| FMTR | Fuel Material Technology Report |
| FT | Fracture Toughness |
| GDC | General Design Criteria |
| GE | General Electric |
| GNF | Global Nuclear Fuel |
| HGC | Hydrogen Gas Cracking |
| HRT | Hydride Reorientation Treatment |
| HT | High Temperature |
| HZP | Hot Zero Power |
| IAEA | International Atomic Energy Agency |
| ID | Inner Diameter |

| | |
|---|---|
| IG | Irradiation Growth |
| IGSCC | Intergranular Stress Corrosion Cracking |
| IPT | Internally Pressurized Tubes |
| IS | Impact Strength |
| ISCC | Intergranualar Stress Corrosion Cracking |
| IZNA | Information on Zirconium Alloys |
| JMTR | Japanese Materials Test Reactor |
| KAERI | Korea Atomic Energy Research Institute |
| LB | Length of Balloon |
| LBLOCA | Large Break Loss Of Coolant Accident |
| LDA | Localized Ductility Arc |
| LEP | Lower End Plug |
| LHGR | Linear Heat Generation Rate |
| LHR | Linear Heating Rate |
| LK | Låg Korrosion (Low Corrosion in Swedish) |
| LME | Liquid Metal Embrittlement |
| LOCA | Loss of Coolant Accident |
| LOM | Light Optical Microscope |
| LVDT | Linear Variable Differential Transducer |
| LWR | Light Water Reactor |
| MCR | Minimum Creep Rate |
| MDA | Mitsubishi Developed Alloy |
| MOX | Mixed Oxide |
| NDA | New Developed Alloy |
| NEA | Nuclear Energy Agency |
| NRC | Nuclear Regulatory Commission |
| NRU | Canadian reactor |
| NSRR | Nuclear Safety Research Reactor |
| NUPEC | NUclear Power Engineering Corporation |
| OBE | Operating Basis Earthquake |
| OD | Outer Diameter |
| OEB | Open End Burst |
| OECD | Organisation for Economic Cooperation and Development |
| OIC | Outside in Cracking |
| OOP | Out of Pile |
| PBF | Power Burst Facility |
| PCI | Pellet Cladding Interaction |
| PCMI | Pellet Cladding Mechanical Interaction |
| PCT | Peak Cladding Temperature |
| PIE | Post Irradiation Examination |
| PL | Pin Loading |
| PNNL | Pacific Northwest National Laboratory |
| PQD | Post-Quench Dutility |
| PST | Plane Strain Tensile |
| PSU | Pennsylvania State University |
| PWR | Pressurised Water Reactor |
| R&D | Research & Development |
| RBMK | Reaktor Bolshoi Mozhnosti Kanalov (in English Large Boiling Water Channel type reactor) |
| RCS | Reactor Coolant System |
| RCT | Ring Compression Test |
| RDA | Rod Drop Accident |
| RIA | Reactivity Initiated Accident |
| RT | Room Temperature |
| RTL | Ramp Terminal Level |
| RTP | Ramp Terminal Power |
| RTS | Ring Tensile Sample |
| RX | Recrystallised |